TRANSDUCTION OF ANTIGENS INTO AMPLIFIABLE DNA SIGNALS USING STRUCTURE SWITCHING APTAMERS

by

Canberk Kayalar

A thesis submitted in partial fulfillment of the
requirements for the degree
of
Master of Science

in

Chemical Engineering

MONTANA STATE UNIVERSITY
Bozeman, Montana

April 2019

ACKNOWLEDGEMENTS

This work was funded by the National Institute of Health's INBRE Program. I would like to thank the Center for Biofilm Engineering for letting me use their equipment and facilities. I would also like to thank Kristen Brileya for training me and Steward Lab workers, who showed me the ropes while using their equipment in their lab. I am happy to have the chance to mentor Marshand Vasquez during his visit to our lab. I am thankful for Matthew Magoon's help in the lab; Matthew, it was a pleasure to work with you. I am grateful for working with Dr. Joseph Menicucci as his teaching assistant, and for his help, time and guidance was much appreciated when I needed the most. Finally, I would like to thank my advisor, Dr. Stephanie McCalla for giving me the opportunity, always having an open door and for her support. She not only thought me a great deal about research and science but an invaluable lesson about adult life of competition and conflict. Of course, without my parents' unconditioned support, this would not be possible. I appreciate my friends Matt and Cory's company who kept me sane throughout this journey.

TABLE OF CONTENTS

TABLE OF CONTENTS CONTINUED

LIST OF TABLES

Table Page

LIST OF FIGURES

Figure Page

LIST OF FIGURES CONTINUED

Figure Page

LIST OF FIGURES CONTINUED

Figure Page

ABSTRACT

Detection of specific antigens has one vital step in common: detection of biomarkers. Diagnostic testing that is rapid and reliable is unavailable in limited resource and rural settings. The solution to this need must be simple, inexpensive, robust, rapid and not require highly trained personnel to operate. Aptamers are capable of delivering those needs when matched with a novel high gain amplification method. This thesis focuses on important aspects of a novel protein detection assay that uses aptamers. Aspects that play an important role on the assay's success were investigated; aptamer selection and design of structure switching aptamers, designing DNA templates that will transduce the signal created by the aptamers, solid phase selection, aptamer immobilization on the solid phase, protein capture, and amplification of the signal. The first step was to find aptamers that were proven to specifically target clinically relevant targets and modify them to suit the needs of the assay. It is important to validate the aptamers' performance. The second important step was finding a solid phase that is compatible with the novel nucleotide amplification reaction that will be used to amplify the signal produced by the aptamers. Paramagnetic microbeads, membranes and polyacrylamide hydrogels were potential candidates for solid phases. Non-specific interaction of the target protein with the solid phase surface will not have negative effects while running the assay due to the structure switching of the aptamers however, it prevented the accurate quantification of the protein capture by aptamers. There is a need for the development of a blocking buffer that is specific to the solid phase. Washing of the excess DNA templates that are not bound to target-bound aptamers plays an important role in the assay's accuracy. The results presented here show the preliminary work that has been done for the novel protein detection assay that uses structure switching aptamers. This assay has the potential to detect diseases at point-of-care in low resource settings.

CHAPTER ONE

INTRODUCTION

Motivation

Treatment of infectious diseases, traumatic brain injury, and cancer has one vital step in common; detection of biomarkers. Diagnostic testing that is rapid and reliable has limited availability and is unavailable in limited resource and rural settings [1]. Lack of proper refrigeration and shipping renders clinical samples useless and adds additional complexity to the problem of accessible healthcare. For example, an on-site diagnostic test for malaria would potentially help to save ~2.2 million lives and prevent ~447 million unnecessary treatments [1]. On the other side, state of the art detection methods also comes with a steep price tag. US spent 17.9% of its Gross Domestic Product (GDP) to health care expenditures in 2016 [2]. Specifically, 2.3% of the GDP in 2013 was spent on *in vitro* diagnostic methods, roughly estimated to be US$ 67 Billion [44].

Limited resource settings often do not allow the use of conventional methods. It is evident that there is a large gap between clinical needs and the current technology. State of the art laboratories can solve these problems; however, these labs are costly and not available in limited resource settings. The solution should be simple and should not require highly trained personnel to operate should be inexpensive, robust and relatively quick.

The answer to this problem lies in an aptamer-based detection assay, that detects antigen-type biomarker molecules. Aptamers are single-stranded oligonucleotides that bind to specific target molecules [4, 5]. Aptamers are competitors of antibodies in regard to their target-specific binding properties. Production of the aptamers is achieved by a procedure named Systematic Evolution of Ligands by Exponential Enrichment (SELEX) [6]. It selects the aptamer that is specific to the target molecule in investigation out of a pool of oligonucleotides [5, 6]. This method permits the non-immunogenic production of aptamers and is easy to scale up when compared with the production of antibodies [3]. Due to their specificity for a wide variety of target molecules and easy production, aptamers make perfect candidates for a point-of-care diagnostic assay for low-income settings.

Current antibody-based methods that are used in antigen detection such as Enzyme Linked Immunosorbent Assay (ELISA) [7, 8] requires multiple washing steps and specialized materials. These requirements hinder its utilization in limited resource settings. Aptamers, when coupled on to a solid phase and utilized as a primer for novel ultra-sensitive DNA amplification reaction [9] will result in an inexpensive and specific assay for its target antigen. Binding aptamers on the solid phase will make washing steps easier and will allow the user to isolate the target-bound aptamers from the sample by simply removing the solid phase. Aptamers have been proven to undergo conformational changes when they bind to their targets [10, 13 and 22]. Aptamers on our assay will

undergo a conformational change and open up its initially closed 3' end (**Figure 1.1**), which will then be utilized as a primer for the amplification reaction that is engineered in our lab [9].

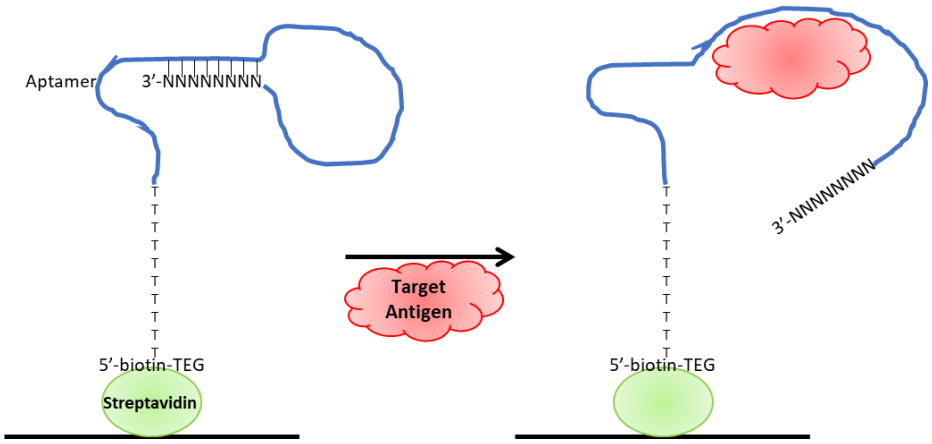

Figure 1.1: Illustration of the opening of the 3' end in the presence of target antigen (not to size). Target antigen is colored red to show that it is fluorescently tagged.

Detecting a wide variety of antigens and being able to accurately diagnose diseases with similar symptoms is an important tool for clinicians [11]. Additionally, the inexpensive and quick nature of the method will allow it to be used in rural areas and in centralized laboratories as an alternative to the current *in vitro* detection methods. This method is better for small molecules with one aptamer binding site. Only single binding event is enough to promote structure switching of the aptamers to initiate amplification.

We focused on clinically relevant targets such as Vascular Endothelial Growth Factor (VEGF), Penicillin Binding Protein 2a (PBP2a) and whole bacterial

cell detection. However, different aptamers are capable of detecting a wide variety of molecules such as cocaine [39] and codeine [30]. This allows the method to be utilized in forensic applications in addition to disease detection.

Enzyme-Linked Immunosorbent Assay (ELISA)

A biomarker is a measurable indicator of a specific biological state, particularly one relevant to the risk of contraction, the presence or the stage of disease [45]. Biomarker detection is a vital step for the treatment of many maladies, from infectious diseases to traumatic brain injury and cancer. Early detection of many cancer types drastically increases the survival rates of the patients [13]. The current gold standard for detection of proteins and antigens is ELISA (Enzyme-Linked Immunosorbent Assay) which uses antibodies to identify a substance. Even though it proved to be the go-to method for detection of proteins for the past 50 years, its applications and availability are limited due to large time, money, and infrastructure requirements to run the test. The requirements prevent ELISA to be utilized as a point-of-care detection method for limited resource settings. WHO characterizes the ideal diagnostics test for low-income areas as, Affordable, Sensitive, Specific, User-Friendly, Rapid and Robust, Equipment-free and Deliverable (ASSURED) [46]. ELISA fails to satisfy some of these criteria to be utilized as a go-to method in the developing world.

Aptamers

Aptamers have previously been utilized in the detection of many clinically relevant targets [15-17]. Conformational changes that aptamers undergo are previously studied [10, 13, 18 and 22] and using aptamers in amplification reactions to generate a signal [31, 32] have proven to be successful. We are combining these advancements together and engineer an assay to diagnose biomarkers that are clinically relevant. While being specific, the proposed assay will be easy to use in limited resource settings and relatively cheap and it will satisfy all of the criteria (ASSURED) WHO requires to be a point of care assay for low-income settings. This assay creates a modular platform for disease diagnostics in an inexpensive manner. There are many options for solid phases. We have chosen magnetic beads, modified cellulose membranes and polyacrylamide gel slugs as potential solid phase supports for aptamers. Furthermore, changing the other components of the assay will result in the adaptation of this method to many applications. We also foresee the application of this assay in an amplification reaction that is taking place in a microfluidic chip that is heated by a simple Proportional-Integral-Derivative (PID) controlled heater or Non-Instrumented Nucleic acid Amplification (NINA). NINA utilizes a proprietary engineered phase change material (EPCM) to maintain a narrow temperature range for isothermal amplification [54].

Aptamer Beacons

Aptamer beacons were utilized as proof of concept for the structure switching capabilities of the aptamers. Aptamer beacons are molecular detection tools that are derived from molecular beacons [22]. The idea behind the molecular beacons is that they give off a signal, in this case fluorescent, when their target is present. Aptamer beacons, in their initial state, have a fluorescent molecule and quencher right next to each other. This significantly reduces the amount of fluorescent signal given out by the beacons before they bind to their target. Binding to the target molecule usually causes the aptamer to switch its structure and results in disassociation of the quencher molecule and fluorophore. This causes an increase in the fluorescent signal when the target binds to the molecular beacon and allows the detection of the target molecule. There are a variety of different designs for aptamer beacons which utilizes either a complementary strand that contains the quencher [50] or aptamers are forced into a hairpin structure by adding a couple of nucleotide long complementary strands on both ends of the aptamers.

Production of Fluoro Targets

To harvest mCherry, E. coli HB101 Biosafety level 1 (BSL 1) with added plasmid MF404 (pMF440, Addgene plasmid # 62550) will be used. E. coli HB 101 was provided by PI Michael Franklin at Montana State University.

E. coli 101 with pMF440 possess multiple traits that is useful. Plasmid MF 440 is a broad host range plasmid for constitutive expression of mCherry. MCherry is a fluorescent protein has a molecular weight of 28.8 kDa. It has a peak fluorescent excitation and emission at 587 nm and 610 nm respectively [23]. Plasmid MF440 also encodes ampicillin resistance, which permits growing E. coli culture in ampicillin added media. Not only this will ensure that overnight culture to only contain E. coli HB101 pMF440, applying antibiotics to the bacteria will ensure the expression of the plasmid and will result in the production of mCherry protein. After growing E. coli, mCherry was harvested by lysing the cells.

Even though mCherry is not a clinically relevant target, it is commonly used in a variety of applications and it is readily fluorescent which eliminates the need for tagging target molecules with fluorescent dyes. Targets other than mCherry require additional preparation step, for making them viable for fluorescent quantification.

Choices of Solid Phase for Heterogeneous Reactions

In order to make this assay easy to use in limited resource settings and wash away any excess assay components, aptamers are immobilized on a solid phase; this is common to all commercially available antigen detection assays. When being utilized in a limited resource setting, the test samples will be mixed directly with the solid phase that already contains the aptamers. Three different

options were investigated for solid supports. These options were magnetic beads, cellulose membrane, and polyacrylamide gels. Each of these options has its own advantages/disadvantages and, manufacturing procedures.

The magnetic beads described here are uniform spherical ferrite particles with a diameter of 1 μm. They have a hydrophilic surface with covalently bound streptavidin molecules. The interaction between streptavidin and biotin is the strongest non-covalent interaction between a protein and ligand [48]. This interaction happens very rapidly, and it is resistant to a wide range of temperatures, pH and buffer conditions.

Cellulose membranes are highly porous filters that are manufactured by overlapping cellulose fibers together. Cellulose strands can be treated chemically with carbonyldiimidazole (CDI) to bind neutravidin on to the cellulose fibers. Neutravidin is another variant of the protein avidin (just like Streptavidin); it possesses the same affinity towards the biotin as the streptavidin, but it has a near-neutral isoelectric point (pI = 6.3). Cellulose membranes are cheap and easy to manufacture, once bounded with neutravidin, they can be stored for 6 months in the buffer. Since they are produced in-house, neutravidin concentration on the surface can be controlled precisely. Due to their porous nature, the surface area of the membrane is bigger than an object with a smooth surface that has the same dimensions. This allows high amounts of aptamers to be immobilized onto the surface without crowding and steric hindrance. In addition to the CDI activated cellulose membrane, a commercial biotin capture

membrane SAM^2 ® Biotin Capture Membrane by Promega (Catalog Number: V2861) was also tested. This membrane is advertised to have a minimal nonspecific binding due to a surface coating.

Lastly, polyacrylamide gels were investigated as a solid phase for the assay. Aptamers can be modified on their 5' end with an acrydite modification, instead of 5’ biotin. This modification allows aptamers to polymerize to the backbone of the gel once it mixes with the catalyzer tetramethylethylenediamine (TEMED). This allows aptamers to be immobilized into the gel directly. Being optically clear, polyacrylamide gels does not interfere with the fluorescence measurements during the amplification step. Polyacrylamide gels can be cast into shapes that favors the diffusion of molecules in and out to prevent the amplification reaction to be diffusion limited.

Signal Transduction and Amplification

Aptamer in their native states will not be able to start the amplification reaction. Aptamers needs to be modified with a 3’ complementary that initially closes the aptamer. Modified aptamers when in the presence of target molecule, will disassociate 3’ end due to the conformational change. This freed up 3’ end can be utilized in a DNA amplification reaction that creates a fluorescent signal. Aptamers were proven to be amplified before using PCR [52] and EXPAR [55]. The amplification method we used is biphasic, switch-like DNA amplification reaction which is similar to the Exponential Amplification Reaction (EXPAR). This

amplification reaction is developed in McCalla Lab, is called Ultra-Sensitive Amplification Reaction (UDAR). UDAR requires a palindromic looped DNA template with two binding domains. Upon loop opening, the oligonucleotide trigger is rapidly amplified through cyclic extension and nicking of the bound trigger [9]. Amplified trigger molecules, after being nicked from the palindromic template, open other palindromic sequences and increases the speed of the amplification reaction. Chemistry of this amplification is isothermal and operates at 55 °C, which simplifies the signal production.

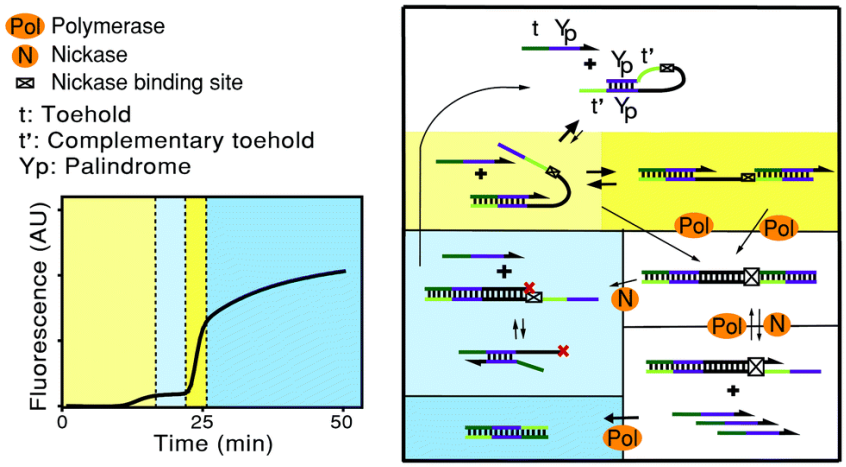

Figure 1.2: Biphasic DNA amplification reaction. The cartoon depicts potential reaction pathways in the biphasic DNA amplification reaction. The amplification requires a looped DNA template with two palindromic sequences (Yp), two toeholds (t′), and a restriction site (⊠), as well as polymerase and nickase enzymes. The reaction amplifies a DNA trigger with a reverse complement to the template toehold (t) and the palindromic region (Yp). Arrows show extendable 3′ ends of the DNA; the 3′ end of the template is blocked with an amine group to prevent non-specific elongation. The trigger can bind to either toehold region t′ and strand displaces the palindromic region Yp, thus opening the loop (yellow). A polymerase can then extend the trigger and create the recognition site for a nicking endonuclease, as well as an identical trigger. The nickase then cuts the

top strand, freeing the newly created trigger to bind other templates. The loop can also remove the long trigger and close with the aid of triggers, which can bind the long trigger and facilitate loop closure. This may be vital to remove “poisoned” long triggers that cannot amplify and block further trigger amplification on the template (light blue). The palindromic region can also cause trigger dimerization, after which the toehold regions can be filled by the polymerase (dark blue); this removes trigger molecules from further amplification cycles. Colored regions on the amplification curve correlate with the proposed dominant reaction mechanism in each reaction phase [9].

The initially closed looped template opens as the newly amplified triggers bind to the looped template. The looped template has 2 trigger binding areas which, both are initially unavailable since it is base-paired to itself (**Figure 1.2**). As the new trigger molecules produced by the amplification reaction and bind to more looped templates, amount of trigger producing sites increases for each trigger that binds to the looped template. Signal outputs were compared for UDAR & other isothermal amplification methods. (**Figure 1.3**).

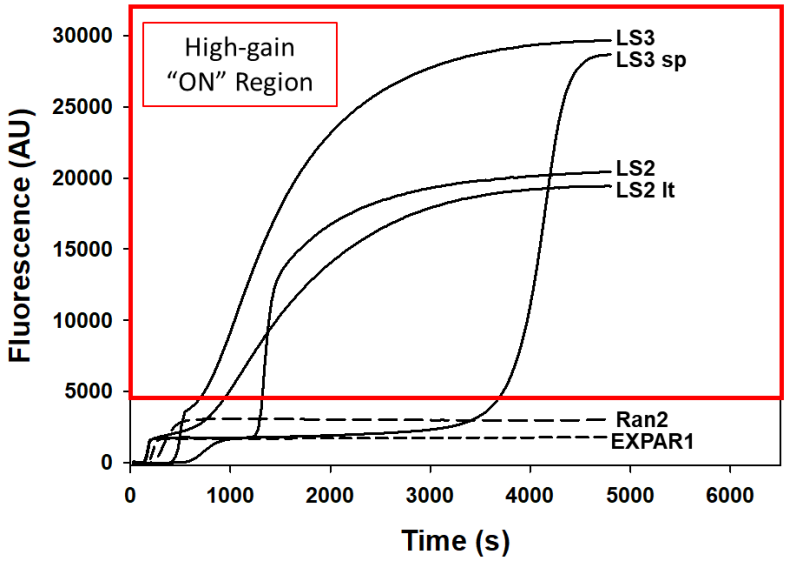

Figure 1.3: Data compares the signal output of the UDAR to a standard isothermal amplification scheme [9].

Goal

The overarching goal of this research is to develop a simple and robust assay for the detection of clinically relevant antigen targets using aptamers that will be a competitor to ELISA. In order to achieve this goal, aptamers with structure switching properties should be designed, and a solid state that is compatible with the amplification reaction and target capture process should be identified and characterized. Having aptamers that switch structures upon target binding are utmost important since it will be the telltale sign of the specific signaling. Solid state that will not hinder the assays ability to work also play an important role on assays success. We used mCherry harvested from E. coli HB101pMF440, Recombinant Human VEGF 165 and PBP2a as our clinically relevant targets. As the aptamers specifically bind to their targets, they will undergo a conformational change, which will be utilized as a primer for a novel high signal amplification reaction [9]. Workflow of the assay is presented in a flowchart shown in **Figure 1.4**.

This method can be utilized in rural areas in addition to low resource settings by utilizing aptamers instead of antibodies. Aptamers have longer shelf stability and cheaper to produce then antibodies. Furthermore, it can replace current protein detection methods as an inexpensive and simple alternative. By replacing the current methods, it has the potential of reducing the cost of diagnosis for a wide variety of diseases and applications. Reducing the cost of detection for such assay will help increase the availability of diagnostics around

the world regardless of geographical and economic boundaries. Lowering the costs also makes it possible for the proposed mechanism to be used as the detection method in generalized laboratories and hospitals. Furthermore, by changing the proposed aptamers with aptamers that are specific to drugs such as cocaine and codeine will make the assay suitable for forensic applications.

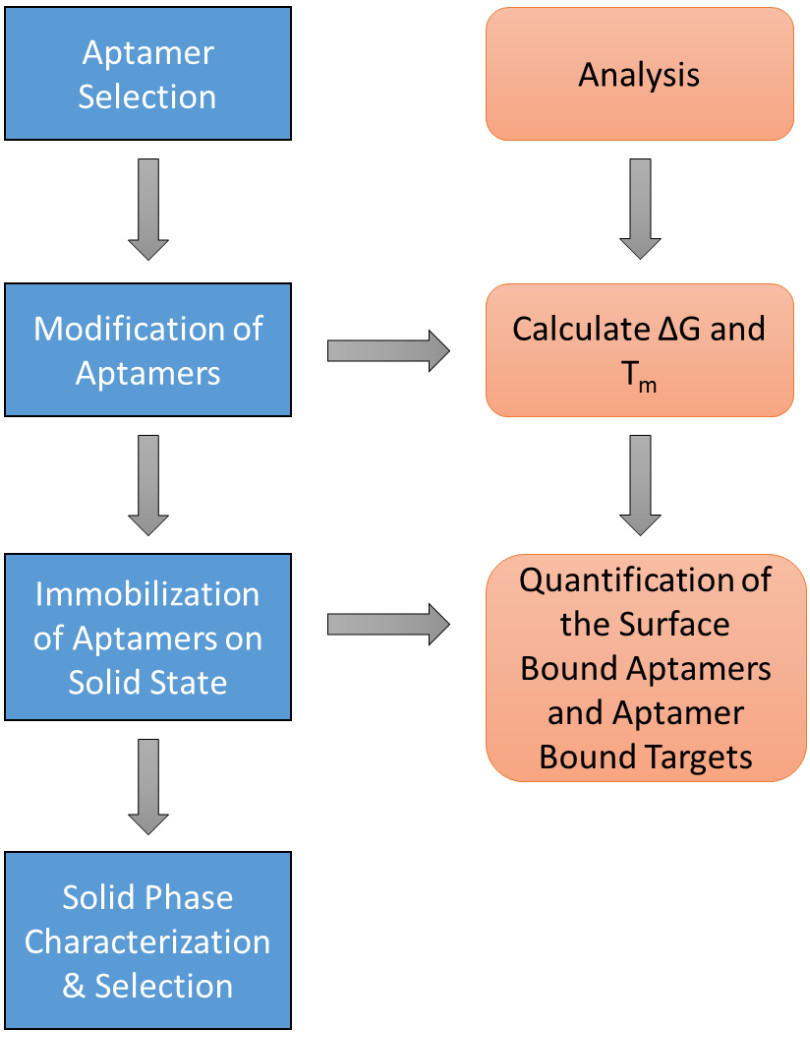

Figure 1.4: Flow chart of the thesis. Each step summarizes the important aspect of the work.

CHAPTER TWO

MATERIALS & METHODS

Aptamer Selection

The first step for engineering this assay was to find well-studied aptamers for clinically relevant targets. The chosen targets are Human Recombinant Vascular Endothelial Growth Factor (VEGF) 165, Penicillin Binding Protein 2a (PBP2a) and mCherry from E. coli HB 101 pMF440. Each of these targets demonstrates a different area of detection. mCherry is a popular molecule used in various applications. VEGF 165 is secreted by the tumors and will demonstrate the assay's ability to bind smaller proteins and as a blood test. PBP 2a will represent the proteins found in the bacteria that are associated with drug resistance.

Aptamers need to be modified in order to fulfill the expectancies of the assay. These modifications will be 5' biotin, 10 nucleotide long T chain (not all of the aptamers have this modification), and 3' complementary sequences to close the 3' end of the aptamers. Aptamers are selected by the method called SELEX [6]. It contains multiple incubating, washing and dissociation steps. Current equipment and interests of McCalla Lab fall outside of conducting SELEX experiments. For this reason, aptamers for the clinically relevant targets such as PBP2a, VEGF and surface antigens of E. coli were either obtained from literature

or purchased. VEGF aptamer sequences were obtained from the literature [36, 37]. PBP2a and mCherry aptamer were purchased from a company specialized on aptamers (BasePair Biotechnologies, INC.).

Modification and Design of the Aptamers

Each aptamer is modified on their 5’ end to either have biotin or acrydite attached to a 10-nucleotide long Thymine chain (poly T spacer). The 3’ end of the aptamers were modified with 7-21 nucleotide long sequences complementary to the aptamer’s protein binding region. This will ensure that 3' ends of the aptamers are closed in the absence of a specific target (**Figure 2.4**). 3' end modifications play an important role in the success and the assay because they allow aptamers to function like a switch. Initially, the modified ends are bound on to the aptamer. After introducing target antigens to the aptamers, the complementary sequence on the 3’ end will disassociate from the aptamers and bind to their target molecule [10]. This dissociation occurs because it is more energetically favorable for the aptamer to bind to their target than the complementary sequence on their 3' end [38-40].

The length of the complementary sequence affects the thermodynamic properties of the aptamer. For the aptamer to bind to its target antigen and disassociate from its 3' complementary sequence, the energy of free binding (ΔG) of the aptamer before binding to its target should be smaller than the ΔG of the aptamer after binding to its target. Melting temperatures (T_m) of the aptamers

are determined by the temperature which amplification reaction runs. Calculations of the ΔG and T_m values for the modified aptamers under specific buffer conditions were made using an online tool called mfold [41-43]. Mfold uses complex equations to calculate the variables in equation presented below. After getting variables ΔH and T ΔS, it solves for ΔG. In addition to thermodynamic properties, mfold will also provide secondary structures for the modified aptamers.

$$\Delta G = \Delta H - T\Delta S$$

Figure 2.1 represents the output mfold gives when aptamer sequence, Ionic conditions, and folding temperature are entered. Ionic conditions and folding temperatures play an important role in the secondary structure of the DNA aptamer [41].

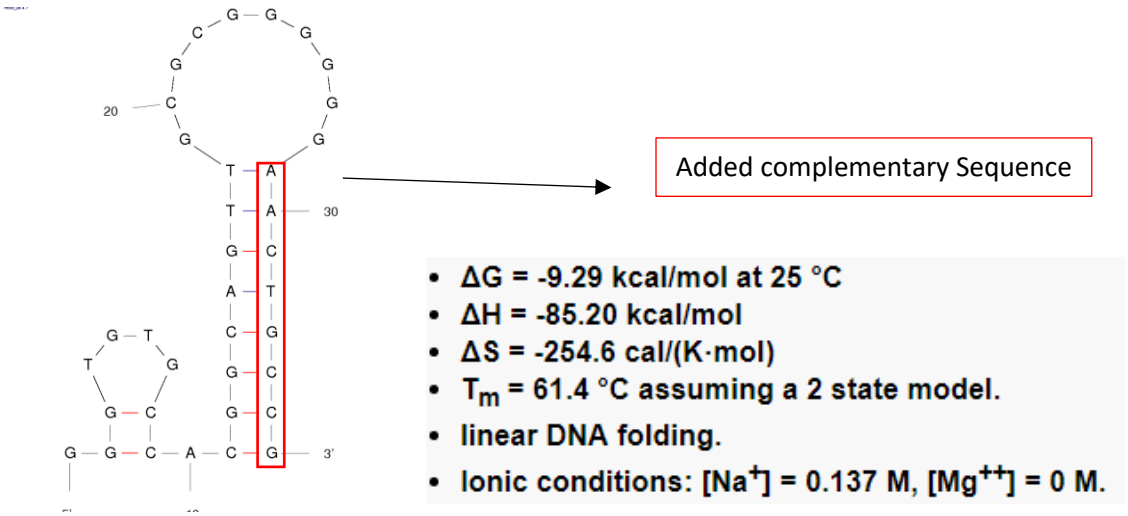

Figure 2.1: Secondary structure and thermodynamic properties of a model aptamer.

Sequences of the PBP2a aptamers are proprietary, however working closely with BasePair Biotechnologies INC., a variety of modified PBP2a aptamers were obtained. CDS0025 is a PBP2a aptamer with no 3' modification while CDS0026, CDS0027, and CDS0028 have complementary sequences with varying lengths in their 3' end that clamps the 3' end of the aptamers to different locations in the aptamer. **Table 2.1** shows the various properties of the aptamers provided by the BasePair Biotechnologies INC.

Table 2.1: Thermodynamic properties and melting temperatures of the secondary structures of the aptamers that were bought from BasePair Biotechnologies and IDT.

Sequence Name	ΔG (kcal/mol)	ΔH (kcal/mol)	ΔS (cal/K.mol)	Secondary Structure Tm (° C)	Nucleotides	Target
CDS0025	-11.4	-115.1	-347.8	57.7	80	PBP2a

CDS0026	-17.92	-177.6	-535.5	58.4	91	PBP2a
CDS0027	-19.01	-167.1	-496.6	63.2	95	PBP2a
CDS0028	-24.83	-190.7	-556.3	69.6	99	PBP2a
CSD0040	-16.8	-176.9	-536.9	56.2	88	PBP2a
CDS0041	-30.35	-220.6	-638.1	72.5	101	PBP2a
GO5	0.43	-17.7	-60.8	17.9	42	mCherry
CDS0035	-17.66	-114.8	-325.8	79.2	57	mCherry
CDS0036	-24.83	-156.3	-440.9	81.3	61	mCherry
Native	-11.41	-96.50	-285.3	64.9	50	VEGF
Option 3	-14.61	-144.10	-434.3	58.6	76	VEGF
Option 4	-12.83	-146.30	-447.6	53.6	78	VEGF
Option 5	-17.85	-175.10	-527.4	58.8	78	VEGF

Aptamers that were obtained from the literature (VEGF Aptamers) were ordered from Integrated DNA Technologies (IDT) with proper modifications that are discussed previously. PBP2a and mCherry aptamers were ordered from BasePair Biotechnologies, INC.

Aptamer Beacons

Aptamer beacons are modified aptamer sequences that creates a signal the presence of a specific molecule. In order to investigate the aptamer's structural switching capabilities, two aptamer beacons that are specific to the

VEGF were designed by modifying a previously reported VEGF aptamer [36]. Native aptamer sequence was modified by adding 5 nucleotides (v5) and 6 nucleotides (v6) long GC clamp on both ends of the beacon to close the sequence to create a stem-loop that is initially quenched, and upon interacting with the target antigen (VEGF) creates a fluorescent signal. Aptamer beacon sequences are (from 5' to 3') 5'- GC clamp sequence, forward primer ATACCAGTCTATTCAATT, aptamer sequence, reverse primer AGATAGTATGTGCAATCA, and GC clamp complementary – 3'. 5' end has 6-FAM (Fluorescein) modification that has the maximum emission at 520 nm and 3' end has Iowa Black® FQ photo quencher. Secondary structures and thermodynamic parameters of the aptamer beacons were obtained using the mfold Web Server [41-43] and structures and sequences are represented in **Figure 2.2** and Thermodynamic parameters are represented in **Table 2.2**.

Table 2.2: Thermodynamic properties and melting temperatures of the secondary structures of the VEGF binding aptamer beacons that are ordered from IDT.

Sequence Name	ΔG (kcal/mol)	ΔH (kcal/mol)	ΔS (cal/K.mol)	Secondary Structure Tm (° C)
v5	-7.66	-145.50	-462.3	41.5
v6	-9.94	-156.10	-490.2	45.2

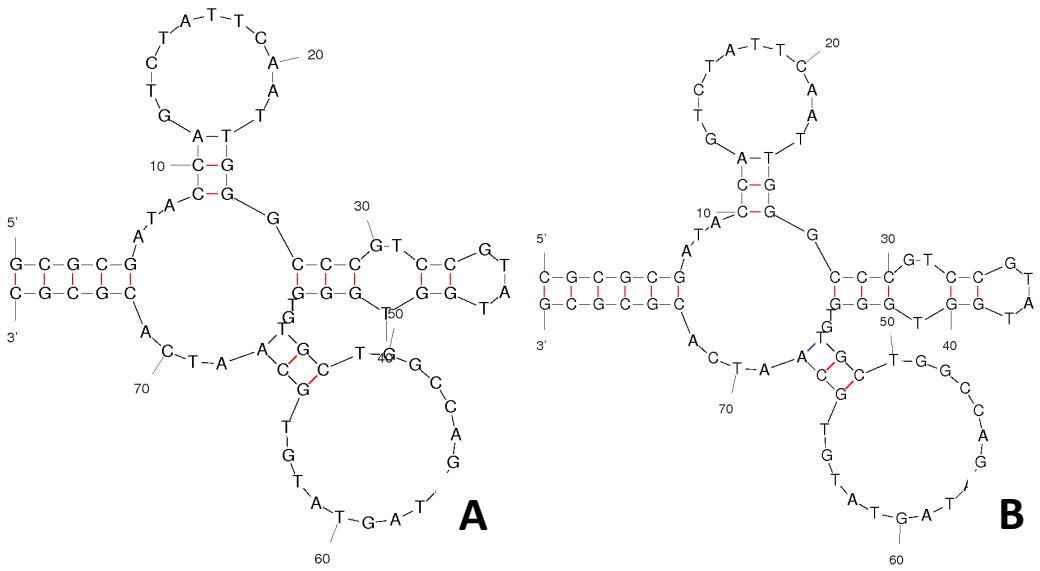

Figure 2.2: Sequences and secondary structures of the VEGF aptamer beacons v5 (A) and v6 (B) that were obtained using the mfold Web Server.

Secondary structures of both aptamer beacons are very similar to each other with the only difference is the length of the GC clamp. Differences in the thermodynamic values are that are represented in **Table 2.2** is mainly due to the 1 nucleotide difference in the clamp. These thermodynamic values were calculated for 25 °C and ionic conditions [Na^{+}] = 0.137 M and [Mg^{++}] = 0 M.

Procedure for the aptamer beacon experiments was as follows: aptamer beacons were spiked into the protein solutions to have the final concentration of 100 nM in all the samples; this results in consistent background fluorescence. Two proteins were tested with the beacons separately; these proteins were, target protein VEGF 165 (R&D systems) and non-specific protein Bovine Serum Albumin (BSA) (VWR). Concentrations of target proteins were ranged from 0 nM

to 500 nM and were diluted in Nuclease Free (NF) Phosphate Buffered Saline (PBS). Fluorescence of the samples was measured using Synergy H1 Hybrid Reader (Biotek) using a 384 well plate (ThermoFisher Scientific). Fluorescence of the samples was measured using the green filter (Excitation: 4850 nm and Emission: 528 nm) for 15 minutes with 1 minute between each measurement.

Immobilization of Aptamers on Magnetic Beads

The first step to running the experiments was the coupling of the aptamers with the Streptavidin coated magnetic beads. Beads that were used was Dynabeads™ MyOne™ Streptavidin C1 beads (Invitrogen). Aptamers were incubated with the streptavidin C1 beads for 30 minutes. This step ensures the coupling of the biotin-tagged aptamers and streptavidin on the surface of the beads.

Since aptamers that were bound to the surface have their own 3D structure, crowding of the surface and steric effects play an important role. The effects of surface crowding on folded and unfolded DNA molecules was shown [19]. When excluded volume effects [20], electrostatic effects [21] and sizes of target molecules are considered, aptamers bound to the surface of streptavidin beads should roughly have 25 nanometers spacing between them. This number is calculated based on the length of a 70-nucleotide long DNA strand by assuming a theoretical length of 3.3 Angstrom (0.33 nm) a nucleotide [47].

After theoretical spacing between aptamers was determined, calculating how many aptamers can fit on the surface of single streptavidin coated bead is possible. Assumptions for this calculation are, each aptamer sits in the middle of a square with side lengths of 25 nanometers, and each Streptavidin beads are perfect spheres with 1-micrometer diameter. With these assumptions we found that roughly 7538 aptamers can fit on the surface of a streptavidin bead that is 1 µm in diameter.

Size of the target antigen plays an important role while determining the amounts of aptamer and streptavidin beads needed for the separation. In this thesis all of the tested target molecules were proteins. **Figure 2.3** illustrates the aptamer molecule that is immobilized on the surface by the biotin-streptavidin interaction.

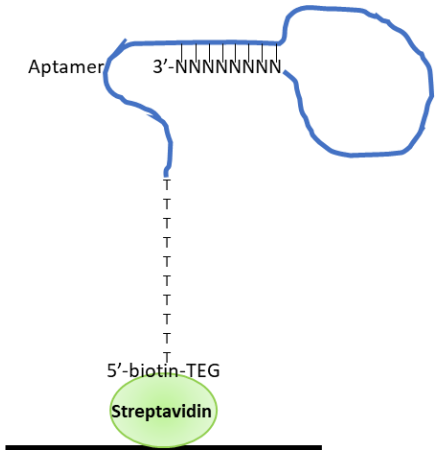

Figure 2.3: Schematics of the immobilization of aptamer on magnetic beads (not to size). NNNN represents the complementary sequence that closes off the 3' end initially.

Aptamers were diluted in NF PBS with 0.01% (v/v) Tween-20 to have the concentration of 100 nM and they were folded using the thermal cycler by heating them to 95 °C for 5 minutes and cooling them back to 25 °C for 15 minutes. This will ensure aptamers to have the desired tertiary structure. After folding of the aptamers, stock bead solution was pelleted using magnetic rack and they were washed in 20 uL of NF PBS once. Beads then were resuspended with the folded aptamer solution and incubated for 30 minutes in room temperature. For every 10 µL of 100 nM aptamer solution, 8.36 µL of C1 beads stock is needed to ensure aptamers are not crowded. After incubation, beads were pelleted using the magnetic rack for 1 minute and the supernatant of this solution was stored to be mixed with equal volume of 2x SYBR Gold (Invitrogen) solution and analyzed using the Synergy H1 Hybrid Reader (Biotek) to determine the concentration of aptamers in the supernatant after incubation.

In House CDI Activated Neutravidin Membrane Manufacturing

In order to attach neutravidin on to the cellulose membrane, cellulose fibers first need to be activated with CDI (Sigma Aldrich) [49]. Whatman qualitative filter paper (Cat #: 1001- 070) was used for this procedure. Filters were cut into smaller rectangular pieces with known dimensions and areas. After cutting the filters into smaller pieces, membranes were washed with gradually increasing acetone concentrations. Initial wash was made in 5 mL of milliQ water to get rid of the water-soluble contaminants on the surface of the membrane. After washing with water, membranes washed in acetone/water solution with

concentrations of 3:7, 5:5, 7:3 and 10:0 respectively. It is utmost important to activate membranes in an anhydrous solvent (acetone) since CDI can be hydrolyzed by water [49]. 0.1981 g of CDI was required for 100 µmoles/cm^{-2} CDI for 2 cm by 6 cm membrane. CDI was first dissolved in 0.5 mL of acetone. The cellulose membrane was added in the 5mL of anhydrous CDI solution and incubated for 2.5 hours while being stirred at 1200 RPM in a round bottom volumetric flask sealed by a rubber septum. After incubation, membranes were washed three times with 5 mL of acetone to wash away any unreacted CDI.

After washing the membranes, CDI activated membranes were dried and immediately coupled with neutravidin. 1uL of Neutravidin stock was diluted in 1 mL of PBS. The 2 cm by 6 cm CDI activated membrane was incubated in the neutravidin solution for 1 hour while being constantly shaken at room temperature. After incubation with neutravidin, membranes were washed with 3 mL of PBS 3 times to remove the unbound neutravidin. After neutravidin treatment, membranes were stored in PBS at 4 °C.

Immobilization of Aptamers on Membranes & Quantification

Aptamers with a 5’ biotin attachment were immobilized on to the cellulose membranes after the neutravidin treatment. Membranes were punched with a circular cutter with a diameter of 3 mm. Stock aptamers were diluted in NF PBS buffer to final dilution of 100 nM with incubated with a single membrane punch. Punches were washed in 10 µL of NF PBS for three times to remove unbound

aptamers. To quantify the amount of aptamer bound on the surface of the membranes, the supernatants were from binding and washing steps were both stored. To quantify bound aptamers, washing supernatants were mixed with a DNA binding fluorescent stain SYBR™ Gold. Any unbound aptamer in the washing fluid would bind to SYBR Gold dye and produce a bright fluorescent signal that can be measured to determine the density of the surface-bound aptamers with the help of a standard curve. The standard curve had 5 points, ranging from 0 nM (blank) to 100 nM aptamer. Unknown aptamer concentrations of the washing supernatants were determined using this standard curve.

Polyacrylamide Gel Production and Casting & Aptamer Quantification

Formulation of the polyacrylamide gel is as follows, 42 µL of DI water, 10 µL of NF PBS, 25 µL of 4x acrylamide/Bisacrylamide (4x AB) solution, 20 µL of 5 µM Aptamer solution and 3 µL of 10% w/v ammonium persulfate (APS) makes 100 µL polyacrylamide gel premix with 1 µM final aptamer concentration. 4x AB is produced by mixing 3.6 mL Acrylamide/Bisacrylamide, 2.58 mL of acrylamide and 3.82 mL milliQ H_2O together and pipetted thoroughly. After the premix preparation, tetramethylethylenediamine (TEMED) solution was prepared by diluting stock TEMED solution in PBS. Final TEMED dilution in the gel slugs were 1:100.

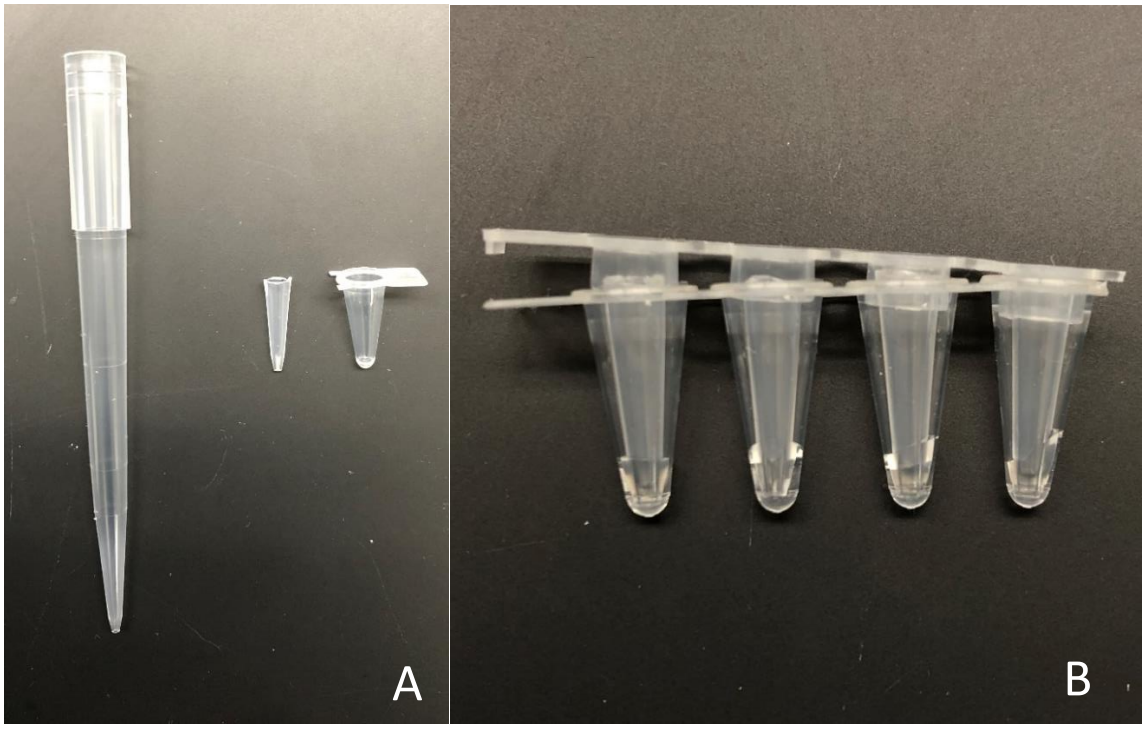

Figure 2.4: (A) shows the pipette tip before and after being cut to fit in the low-profile PCR tube. (B) shows how pipette tips sits in the low-profile PCR tube when capped. Polymerized gel slugs can be seen in the bottom of the tubes.

The casting of hollow polyacrylamide gel slugs required a make-shift cast that is made by inserting a pipette tip inside of a low-profile PCR tube. The tip of the pipette was cut so that when it was placed inside of the low-profile PCR tube, it was sitting flush with the tube (**Figure 2.4 A**). This allowed the tube to be capped and hold the tip in place and not move around during the centrifugation step (**Figure 2.4 B**). After cutting the pipette tips and placing them inside of the low-profile tubes, 9 µL of aptamer premix was loaded in the space between the pipette tip and low-profile PCR tube. After being capped, they are centrifuged at 3000 x G for 30 seconds to allow the premix to collect at the bottom of the tube,

around the pipette tip. After centrifugation, 1 µL of 1:10 diluted TEMED was added in the same manner as the premix, then centrifuged. After this centrifugation, tubes were left undisturbed for 1 minute to allow the gel to be polymerized. After 1 minute, caps and the tips were carefully removed without disturbing the hydrogel using a tweezer. (**Figure 2.5**).

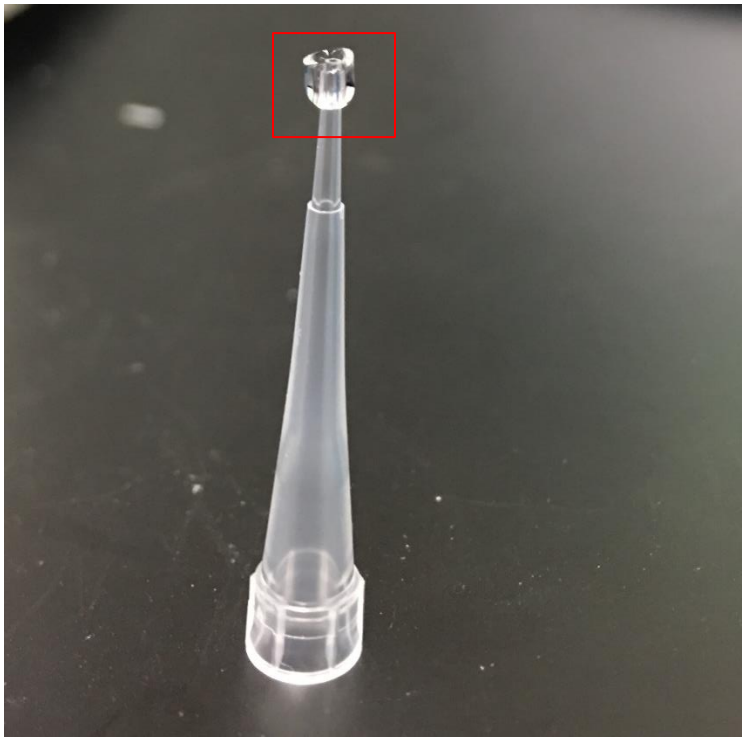

Figure 2.5: Hollow polyacrylamide gel that carefully taken out of the low-profile PCR tube and placed on top of a 10 µL pipette tip. Tip of the pipette tip runs thru the channel that is in the middle of the poly acrylamide slug.

Next step was washing the slugs with NF PBS, 20 µL of NF PBS was added into the slugs and pipetted carefully to ensure mixing. 10 µL of this washing supernatant was pipetted out and mixed with 10 µL of 2x SYBR Gold

solution. A standard curve with 6 varying DNA concentrations (points) was made. These points were 250 nM, 200 nM, 150 nM, 100 nM, 50 nM and 0 nM. For each standard curve point, 10 µL of 2x concentration of that point is mixed with 10 µL of 2x SYBR Gold Solution. All dilutions are made with NF PBS.

Production of Fluoro Targets

MCherry:

E. coli HB 101 were grown in Stewart Lab. Stock E. coli was stored in a -80 °C freezer in suitable conditions [24]. It was shown earlier that E. coli strain that is very closely related to the E. coli HB101 is grown using LB broth at 37 °C [25]. However, previous experience with E. coli HB101 shows Tryptic Soy Broth (TSB) and Tryptic soy agar (TSA) with ampicillin also supports growth of E. coli HB101 in 125 mL baffled Erlenmeyer flasks overnight.

Due to the reduced activity of ampicillin in older ampicillin plates [26], E. coli were streaked to a fresh ampicillin plate every month. E. coli HB101 has a bright red color under optimal conditions due to the presence of mCherry fluorescent protein. Bacteria on the streak plates that are older than 1 month starts losing its bright red color, which is a of plasmid loss in the colonies. It is possible for bacteria to lose their plasmids [27, 28] when the plates streaked with E. coli that are older than 1 month. Overnight cultures inoculated from these

plates results in a colony that is completely yellow, showing drastically reduced mCherry levels.

After growing the overnight culture, bacteria were centrifuged for 2 minutes at 8000 x g to pellet the bacteria at the bottom of the tube. After pelleting the bacteria, the media was replaced by PBS. To harvest the mCherry proteins that were inside of the E. coli, E. coli cells needed to be lysed. Cells were lysed using a sonicator: 10 mL of E. coli that is resuspended in PBS were sonicated for a total of 10 minutes at 11 Watts. To prevent overheating the sample, the 15mL falcon tube that was holding the bacteria was placed in an ice bath and the sonicator was powered for 10 second intervals with 10 seconds cooldown between sonication. After sonication, the solution was centrifuged to pellet the cell debris and supernatant was moved into a new Falcon tube. Additionally, the solution was filtered using a syringe filter (Millipore Cat # SLMP02SS) with 0.22 µm pore size to further ensure that there were no bacteria in the mCherry solution.

Fluorophore Labeling:

Human Recombinant VEGF 165 (R&D Systems) and Recombinant S. aureus PBP2a (Ray Biotech) were labeled with a fluorescent dye. Alexa Fluor™ 594 (Invitrogen) has excitation/emission values of 590/617 nm which is close to mCherry and has a bright red color and Alexa Fluor™ 488 (Invitrogen) with excitation/emission values of 495/519 nm and is a green fluorophore. Target proteins VEGF 165 and PBP2a were labeled with the fluorophores according to

the manufacturer's instructions using Alexa Fluor™ 488 Microscale Protein Labeling Kit (Invitrogen).

Depending on the reaction volume, protein fluorescence was measured by Synergy H1 Hybrid Reader (Biotek) or NanoDrop™ 3300 Fluorospectrometer (ThermoFisher Scientific).

Designing Transduction Templates

Transduction templates contain 3 sequences that play an important role in the amplification. From 5' to 3' these sequences are, reverse complement of a reporter oligonucleotide (LS2), nickase recognition site and complementary sequence to the opened up 3' end of the aptamer. Nickase frees the newly extended reporter sequence and drives the high gain autocatalytic amplification of the reporter sequence. **Figure 2.6** illustrates the transduction templates and how they interact with the opened 3' end of the modified aptamer. Additionally, transduction templates also contain a 3' amino modifier so that they can not be extended on the 3' end by the DNA polymerase.

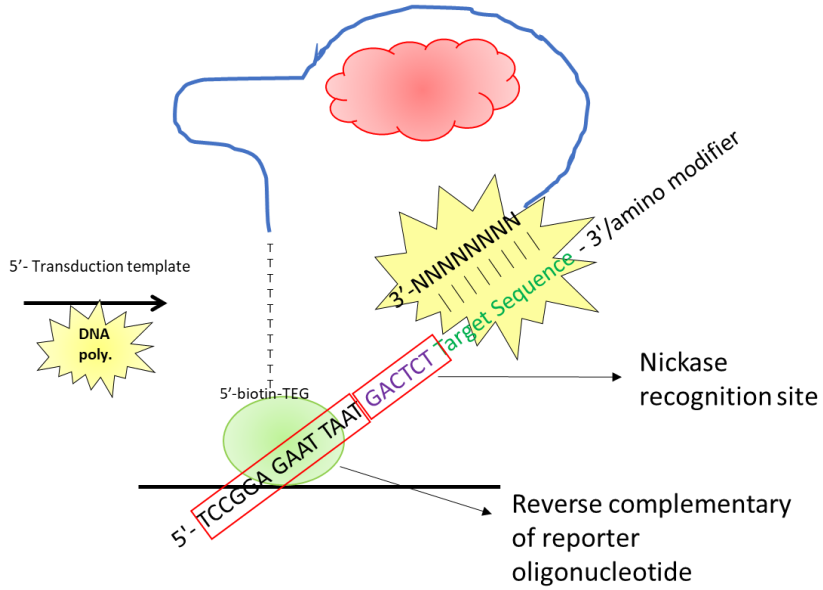

Figure 2.6: Schematic of how transduction templates interact with the open 3' end of the modified aptamer.

Transduction templates that bind to modified PBP2a and mCherry aptamers were ordered from BasePair Biotechnologies. Secondary structures, melting temperatures, thermodynamic properties and target aptamers of the transduction templates are presented in **Table 2.3**

Table 2.3: Melting temperatures of the secondary structures, thermodynamic properties and target aptamers of the transduction templates that were purchased from BasePair Biotechnologies.

Sequence Name	ΔG (kcal/mol)	ΔH (kcal/mol)	ΔS (cal/K.mol)	Secondary Structure Tm (° C)	Nucleotides	Target (CSD/OP)
CDS0030	-3.23	-44.8	-139.4	48.1	31	26
CDS0031	-4.68	-48.6	-147.3	56.7	35	27

CDS0032	-5.42	-60.7	-185.6	54.2	39	28
CDS0038	-2.29	-43.6	-138.5	41.5	35	35
CSD0039	-2	-43.6	-139.5	39.3	39	36
CDS0042	-1.65	-33.3	-106.1	40.5	28	40
CDS0042	-2.33	-64.5	-208.5	36.1	41	41
Td Native	-2.36	-36.90	-115.8	45.3	30	Native
Td Op 3	-1.27	-37.70	-122.1	35.3	30	Option 3
Td Op 4	-0.89	-31.10	-101.3	33.7	32	Option 4
Td Op 5	-3.37	-44.20	-136.9	49.6	32	Option 5

Amplification Reaction

Ultra-Sensitive DNA Amplification Reaction (UDAR) [9], is an isothermal amplification reaction engineered in our lab that has hill type kinetics (**Figure 1.3**). Hill type kinetics allow this reaction to produce a high signal output. For initial experiments, aptamers that were incubated with the target molecule were mixed with the transduction templates and amplified using UDAR. The first set of experiments tests the association of the aptamers and transduction templates and therefore aptamers were not immobilized on a solid phase.

The amplification reaction mixture contained 1× ThermoPol I Buffer [20 mM Tris-HCl (pH 8.8), 10 mM (NH4)2SO4, 10 mM KCl, 2 mM MgSO4, 0.1%

Triton® X-100], 25 mM Tris-HCl (pH 8), 6 mM MgSO4, 50 mM KCl, 0.5 mM each dNTP, 0.1 mg/mL BSA, 0.2 U/µL Nt·BstNBI, and 0.0267 U µL−1 Bst 2.0 WarmStart® DNA Polymerase. Bst 2.0 WarmStart® DNA polymerase is inactive below 45 °C; this decreases non-specific amplification before reaction initiation and theoretically increases experimental reproducibility [9]. Transduction templates, aptamers and target protein (PBP2a) were diluted in PBS and added at a final concentration of 10 nM. SYBR Green II (10,000× stock in DMSO) was added to the reaction mixture to a final concentration of 5x. Reactions were prepared at 4 °C, and aptamers, target proteins, and transduction templates were handled in separate hoods and benches to prevent contamination. For each experiment, three controls were prepared: a "blank" with a reaction mix only, a sample containing no target protein, and a sample with a non-specific transduction template. Reactions were run in triplicates with 20 µL volumes. Fluorescence readings were measured using a BioRad CFX Connect Thermocycler (Hercules, CA). Measurements were taken every 20 seconds with a 12 second imaging step, and therefore reactions were run for 150 cycles of 32 seconds at 55 °C. The mixture was heated to 80 °C for 20 minutes to deactivate enzymes, followed by 10 °C for five minutes to cool the samples. Data were analyzed using a MATLAB code that background corrects the data and calculates the inflection points.

Readout of this assay is the short DNA sequences that called reporter molecule (LS2) produced by the UDAR. First sets of reporter molecules are

amplified using the transduction templates (**Figure 2.6**). Production of reporter molecules leads to a cascade of reporter molecule production: reporter molecules bind to the 3’ end of the looped templates, which contain the reverse complement of the 5’ end. Each reporter molecule associating with a looped template will therefore create a new reporter. Details of the biphasic, high gain reaction mechanics were given in **Figure 1.2**.

CHAPTER THREE

RESULTS & DISCUSSION

Aptamer Beacons

Aptamer beacons v5 and v6 have a complementary sequence on their 5’ end that clamps the 3' and 5' end of the aptamer beacons together. Clamping of the 3' and 5' ends of the beacons results in a low initial fluorescent signal due to the FRET interaction of Fluorescein and Iowa black photo quencher. Expected results for the beacons was to observe an increase in florescence of the samples with the addition of the target molecule VEGF since they were to undergo a structural change after binding to their target molecule. This leads into the opening of the GC clamp that would lead into the separation of the 5' Fluorescein and 3' Iowa Black photo quencher which would result in an increase in fluorescence of the samples. However, over the 15 minutes, beacons did not yield in a significant increase in fluorescence of the samples and as the protein concentrations increased, the fluorescence of the samples reduced significantly. **Figure 3.1** shows fluorescence values averaged over 15 minutes for each protein concentration; fluorescence measurements were taken 1 minute apart, a total of 16 measurements plotted in a fluorescence vs. protein concentration graph.

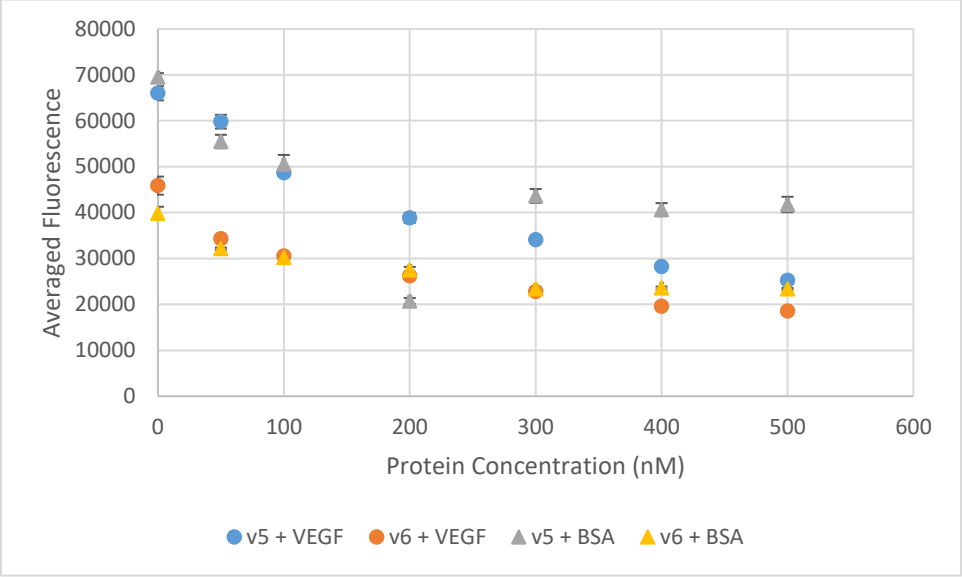

Figure 3.1: Average fluorescence of the aptamer beacons with various protein concentrations. Sample's fluorescence had measured each minute for 15 minutes then averaged and plotted against protein concentration.

For both proteins, specific (VEGF) and non-specific (BSA), increasing protein concentrations resulted in lower fluorescence values compared to the low protein concentrations' fluorescence values. This was the most interesting outcome of this experiment since there was no significant increase in fluorescence over 15 minutes in VEGF (specific protein) samples. There was a slightly decreasing trend when Fluorescent vs Time graphs were plotted for VEGF (not shown here) which most likely caused by photobleaching after each consecutive measurement.

Currently, the aptamer binding region is flanked by random primer sequences. For future experiments, new aptamer beacons should be designed with a complementary sequence that would base pair close to or on the

aptamer's target binding domain. This will ensure that when aptamer interacts with the target, it will dissociate the complementary sequence hence increasing the likelihood of observing the structural change that aptamers undergo.

Evaluation of Solid Supports

Characterizing Diffusivity of Reagents Through Hydrogels:

As they are optically clear and capable of polymerizing aptamer molecules directly on the backbone of the gel by adding a 5' acrydite modification to the aptamers, PA gels are a viable option for a solid support. There are 2 parameters that mainly affects the performance of the polyacrylamide gel slugs, diffusion of reagents through the gel matrix and the ability to work with the amplification method UDAR. In order to demonstrate the diffusion of the reagents, cylindrical gel slab with 3 mm height and 25.36 mm diameter was casted and incubated in 1 µM Fluorescent Neutravidin (diluted in 1:10 PBS) overnight. After incubation, gel slab was placed in 2 mL of PBS diluted in NF water 1:10. 1:10 PBS is used to match the salt concentration that is present in the gel slab so that osmotic pressure does not cause swelling or shrinking of the gel and there is the only diffusion of proteins and not convection. The gel slab was incubated in 1:10 PBS for 20 minutes at room temperature and every 2 minutes, 10 µL samples were removed from the solution. This resulted in 10 measurements over 20 minutes and 100uL of washing buffer removed from the 2 mL total volume. Effects of the volume decrease are assumed to be negligible; to prevent further volume loss by

evaporation, the container was covered with parafilm throughout the process. To ensure the concentration of protein in solution was homogenous, the experimental setup was shaken gently. Concentration of the neutravidin in the washing buffer with respect to time using Nanodrop-3300 at wavelength 518 and the standard curve is presented in **Figure 3.2**.

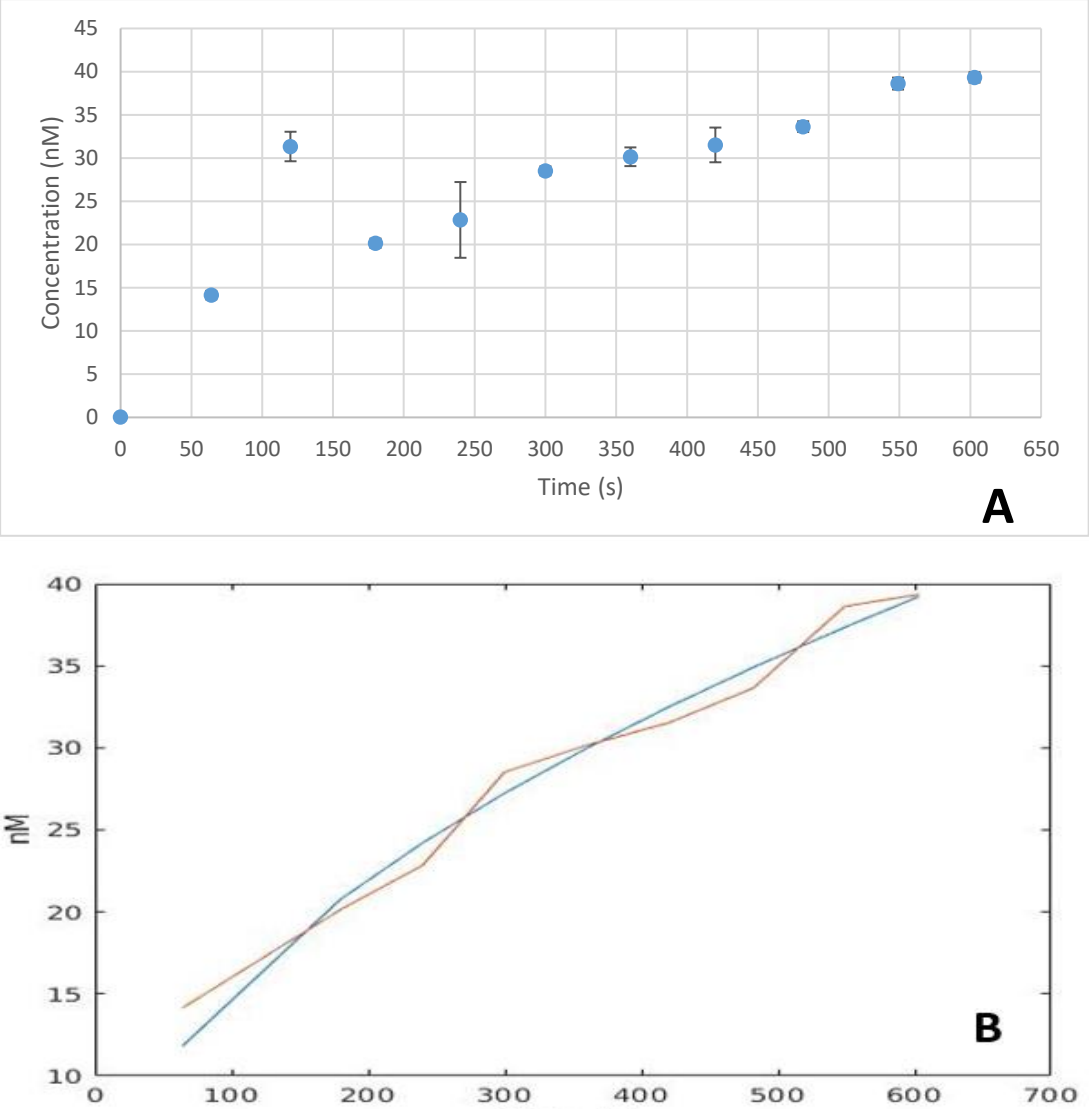

Figure 3.2: (A) Change of concentration of the washing buffer with respect to time. (B) Diffusion model that was that was fit to the concentration data

presented at (A). Blue line represents the model and red line represents the measurements.

Third data point (t = 2mins), is unusually high and is assumed to be an outlier. After 10 minutes, the concentration of Neutravidin in the supernatant was 39.3 nanomolar. The pore size of the gel provides insightful information about the capabilities of protein diffusion and porosity is a key parameter that is used to calculate the PA gel's diffusivity. The porosity of the polyacrylamide gel was determined by drying out a 250 µL gel slug overnight and measuring the wet and dry weight of the gel slug. Difference between dry and wet weight correspond to the water that was in the pores and dividing the dry weight to the wet weight gives the porosity of the PA gel. Wet weight of the gel was measured to be 263.1 mg and dry weight was 18.9 mg; porosity of the gel is roughly 92.8%. The pore size of the gels is a function of total monomer concentration (%T) and the weight percentage of crosslinker (%C) [51]

$$\%T = \frac{gram\ acrylamide + gram\ crossliner}{Total\ volume, mL}\ x\ 100$$

$$\%C = \frac{gram\ crosslinker}{gram\ acrylamide + gram\ crossliner}\ x\ 100$$

%T was calculated 10.28% to be and %C was 8.65%. This %T and %C values corresponds to ~ 25 nm pore radius [51].

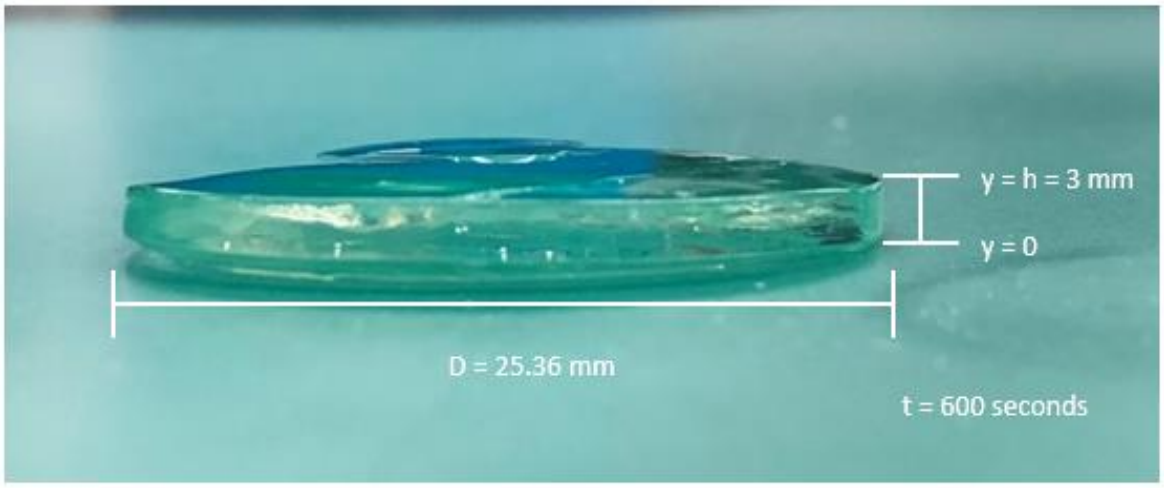

Figure 3.3: Side image of the actual PA gel slab used in the experiment. Gel slab was casted to have height of 3 mm and diameter of 25.36 mm. Pa gel slab was left in the washing buffer for 10 minutes (t_{final} = 600 secs). Bottom and sides of the gel slab was confined in a thigh fitting container and washing buffer was sitting on top of the gel slab.

To determine the diffusivity of proteins through the hydrogel matrix, we have fit the above data (**Figure 3.2**) to a partial differential equation model. Initial condition for the model was taken as C (t≤0, y) = C_0 and boundary conditions were C (t>0, y=h) = C_1 and no flux boundary condition $-D\ \frac{\partial C}{\partial y} = 0\ (@y = 0)$. The governing partial differential equation was:

$$\theta = 1 - 2\sum_{n=0}^{\infty} e^{[-\left(n+\frac{1}{2}\right)^2 \pi^2 \tau]}\ \cos[(n+1/2)\pi\eta]\frac{(-1)^n}{(n+\frac{1}{2})\pi} \qquad \text{Equation 3.1}$$

Where;

$\theta = \ (C - C_0)/C_1 - C_0, \eta = y/h, \tau = \frac{tD}{h^2}$

Diffusion was assumed 1D, through the top surface of the gel (y = h, η = 1) and flux is:

$$N = -D\frac{\partial C}{\partial y} = -D\ \frac{(C_1 - C_0)}{h}\frac{\partial \theta}{\partial \eta} \qquad \text{Equation 3.2}$$

using the equalities $C = \theta(C_1 - C_0) + C_0$ and $y = h\eta$. When ***Equation 3.1*** is plugged into ***Equation 3.2*** and solved for $\eta = 1\ (y = h)$ we obtain:

$$N(@\, y = h) = \frac{-2D(C_1 - C_0)}{h}\sum_{n=0}^{\infty} e^{\left[-(n+\frac{1}{2})^2\pi^2\tau\right]}$$

When this result is further integrated from t=0 to t_1 and units converted to moles/L we obtain,

$$C_{Solution} = \int_0^{t_1} N dt * \frac{A}{V} = \frac{A2h(C_1 - C_0)}{V}\sum_{n=0}^{\infty}\frac{1}{(n+\frac{1}{2})^2\pi^2}\left[e^{\left[-(n+\frac{1}{2})^2\pi^2\frac{Dt_1}{h^2}\right]} - 1\right]$$

Where A is the area of the top surface of the gel and V is the volume of the solution above the gel slab.

Diffusivity of the neutravidin through the PA gel slab was calculated to be 3.89 x 10^{-11} m^2/s using the best fit of the equations presented above to the data. Diffusion of neutravidin was modeled using MATLAB (**Figure 3.2 B**). Blueline shows the model and red line show the measured values. A similar study that investigated the diffusion of a similarly sized protein (BSA) in PA gel reported the diffusivity of the BSA to be 6 x 10^{-11} m^2/s in a 2.7% crosslinked PA gel [53]. Slight

difference between two values is due to a slight difference in the protein size (neutravidin is 7K Da bigger) and PA gel compositions. Overnight incubation of polyacrylamide gel slab in neutravidin was not enough to reach steady state and could not reproduce the initial condition. However, result obtained is likely to be similar to real value because a short observation time frame (10 mins) resulted in small perturbation of the top layer only, which was at $C = C_0$. Future work will replicate this experiment after hydrogel has been equilibrated for a greater time period ($\tau \geq 2$).

DNA Binding Densities:

DNA (aptamer) binding capabilities of the solid phases will be discussed in this section. Each of the four solid phases that were used has different DNA binding capabilities and characteristics. These solid phases are Dynabeads™ MyOne™ Streptavidin C1 beads, In-house (CDI) membrane and commercial membrane (SAM2 Biotin Capture) and, polyacrylamide gels.

C1 Streptavidin Beads:

Dynabeads™ MyOne™ Streptavidin C1 beads' performance for capturing aptamers were quantified using Nanodrop 3300 Fluorospectrometer. Out of the 3 options, C1 beads were the best performing option for DNA (aptamer) immobilization due to their high % DNA capture abilities, low incubation time (15-30 mins) and ability to hold on to bound aptamers after washing steps. **Figure**

3.4 shows the percent of aptamers that were immobilized to the surface of the C1 beads; the same experiment was run 3 times on different days and percent immobilization of aptamers was averaged for each aptamer. Initial aptamer concentrations were 100 nM and C1 beads were incubated in the aptamer solution for 30 mins. After Incubation, C1 beads were pelleted using a magnetic rack (1 minute) and supernatants were taken to a new tube. An equal volume of 2x SYBR® Gold was added to samples and they were quantified using NanoDrop 3300 at 537 nm wavelength. After immobilization, aptamers were placed in 20 µL of NF PBS containing 0.01% TWEEN and incubated in this buffer for three and a half hours. After this extensive wash, 5 µL of supernatant was taken out and it was mixed with equal volume of 2x SYBR® Gold and quantified as discussed in the methods section.

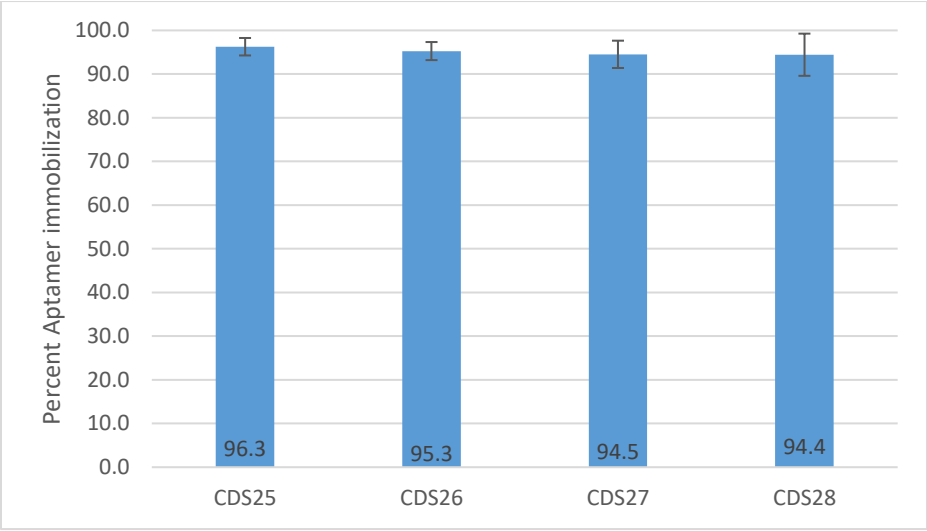

Figure 3.4: Percentages of aptamers immobilized on the C1 beads are represented in this bar chart. Four different aptamers with 5' biotin attachments were incubated with the beads on 3 different days and averaged.

DNA concentrations in the washing supernatants (not shown) were very low. This suggests that aptamers are stably bound they stay immobilized even if the beads are washed.

Cellulose Membranes:

DNA immobilization capabilities of in-house membranes and commercial membranes are dramatically different from each other. Percent of aptamers (CSD0025, CDS0026, CDS0027 and CDS0028) immobilized on to the membranes were presented in **Figure 3.5 A**. Concertation of aptamers that were left in the supernatant after incubation were calculated using the standard curves in **Figure 3.5 B**.

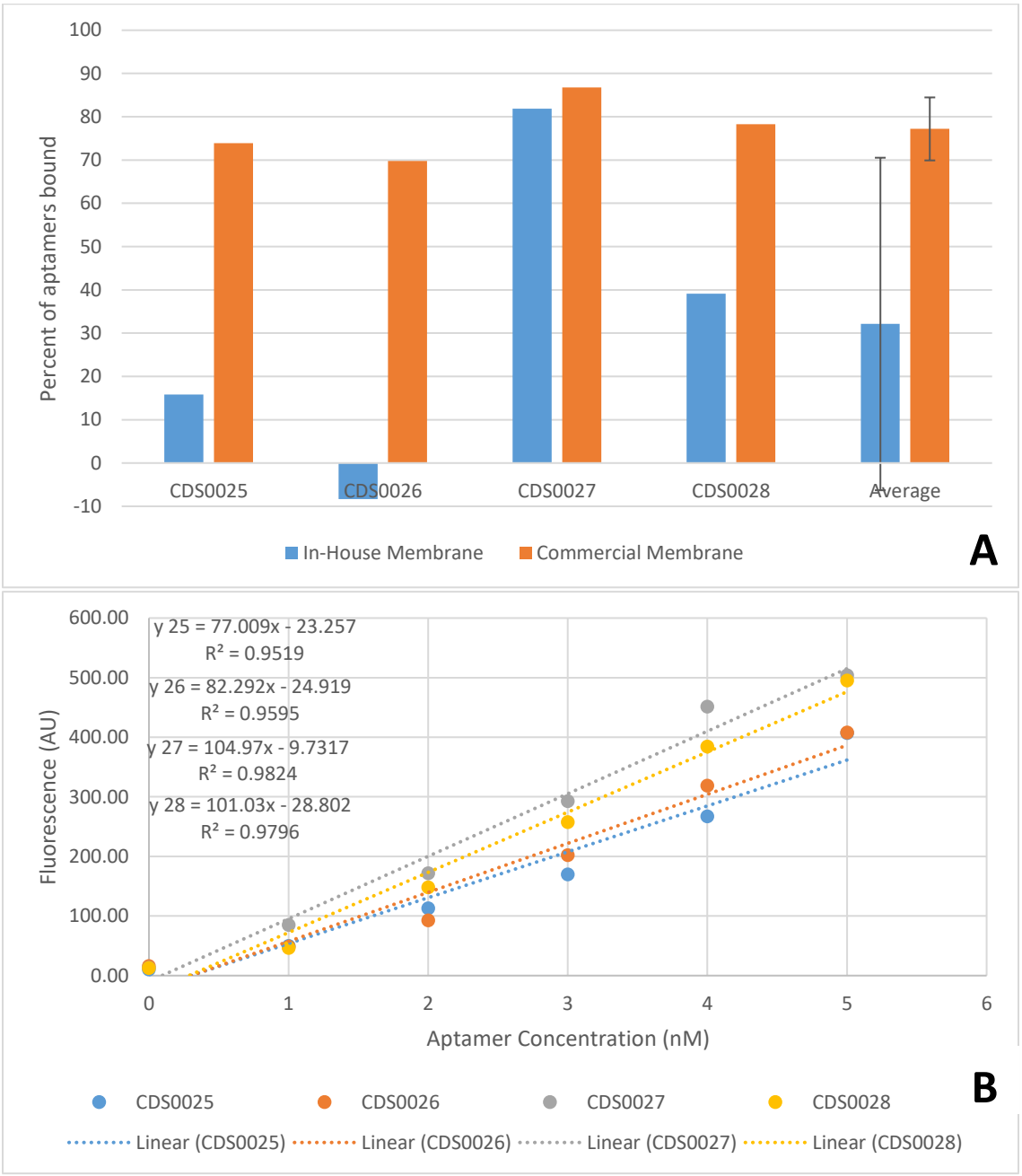

Figure 3.5: (A) Percent of the aptamers immobilized on the membranes. (B) Standard curves of the aptamer immobilization data. Linear regression was used to calculate the aptamer concentrations that are left over after incubation using the corresponding standard curves presented here.

Percent aptamer immobilization ranged from -8.3% to 81.9% for In-house (CDI-Neutravidin) membranes and Commercial (SAM2 Biotin Capture) membranes resulted in a more uniform range from 69.8% to 86.8%. Looking at the average percent of aptamers immobilized on the membranes, In-house membranes had 32.1 ± 38.4% immobilization and commercial membranes had 77.2 ± 7.3% of the aptamers immobilized on them after incubation. It is evident that there is large variability between In-house membrane samples. This could be due to the non-homogenous neutravidin concentration on the surface or any other inefficiencies during In-house membrane production.

We have previously observed cellulose strands that were shed by the in-house membranes during in the incubation period, which then nonspecifically interacts with the SYBR Gold and results in increased fluorescence. RFU values of the Blank supernatants suggest a similar trend with this theory. Blank supernatant for In-house membrane had RFU of 129.7 and Commercial membrane resulted in an RFU of 13.7. When compared to the standard measurements, RFU of 13.7 is close to 0 nM of DNA while 129.7 is on roughly around 2 nM. This suggests non-specific adsorption of SYBR Gold to the Cellulose membranes. For this reason, commercial membranes (SAM2 Biotin Capture Membranes) are more viable then the In-house membranes.

Polyacrylamide Gels:

A standard curve was used to calculate the DNA concentration in the gel slug supernatants (**Figure 3.6**) and results of the immobilization is represented in **Figure 3.7**. Percent aptamer bound for each gel slug replicate was calculated by subtracting the concentration aptamers that are in the washing supernatant from the initial concentration of aptamers that are in the gel slug and normalizing it and multiplying it with 100.

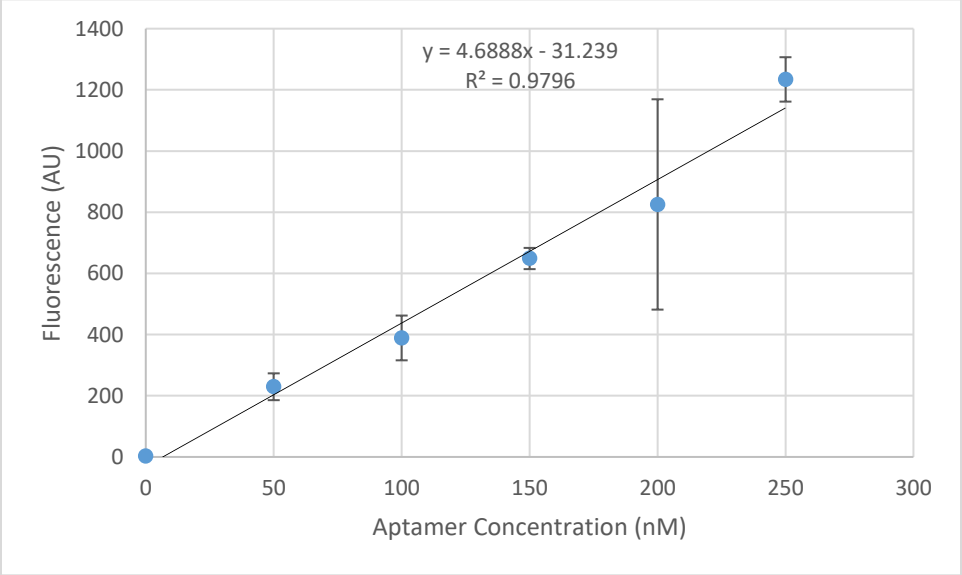

Figure 3.6: Standard curve that is used to calculate the aptamer concentration of the washing supernatant of the hollow gel slugs.

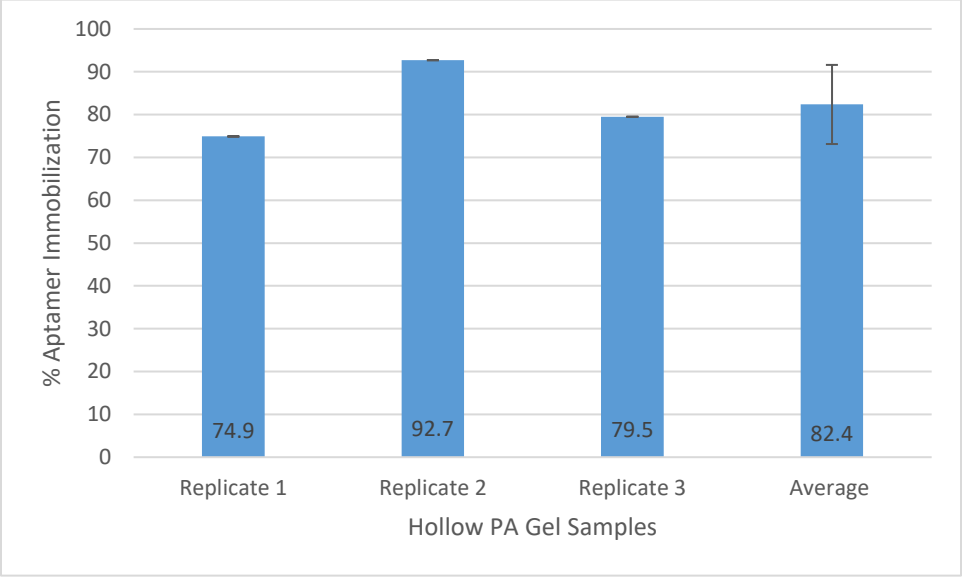

Figure 3.7: Percent of aptamers that are bound to hollow PA gel slugs.

The average percentage of aptamers in the polyacrylamide gel slugs are 82.4 ± 9.18%. After Aptamer Quantification, leftover washing supernatant was analyzed with NanoDrop 1000 to see if there are any other substances in the washing supernatant. Data of this measurement is presented in **Table 3.1**.

Table 3.1: Shows the ratio of absorbance at 260 to 280 nm and 260 to 230 nm. These values show the purity of the samples.

	A260/A280	Standard Deviation	A260/A230	Standard Deviation
Replicate 1	9.48	0.25	0.82	0.07
Replicate 2	5.38	1.08	0.04	0
Replicate 3	7.93	0.23	0.27	0.02

Looking at the A260/A280 values for the washing supernatants of the samples, they are higher than the standard value of ~1.8 for DNA. A260/230 values are substantially lower than its standard values 1.8-2.2. Having high A260/A280 and low A260/A230 shows that washing supernatants contain contaminants alongside washed of DNA. Polyacrylamide gel slugs bleed chemicals and need to be washed thoroughly. Next logical step was to investigate if the chemicals that are bleeding out of the polyacrylamide gel slugs are inhibiting the reaction. While testing this, other solid phases' compatibility with the UDAR reaction will be also tested.

UDAR Compatibility of the Solid Phases:

Four solid phases, membranes (In-house and commercial), Streptavidin C1 Dynabeads™ and hollow polyacrylamide gel slugs were placed inside the UDAR reaction that amplifies the trigger miRNA-223-3p using the exponential template LS2 and Linear template miR223LS2. This is a template that has been proven to amplify micro RNA 223. 3 mm punches of in-house (CDI) membranes and Commercial membranes, 9.55 x 10^5 beads/20 µL C1 Dynabeads™, hollow polyacrylamide slugs that were washed in 100 µL of Tris-EDTA (TE) buffer 3 times and conditioned in 100 µL NEBuffer™ 3.1 overnight and unwashed hollow polyacrylamide slugs were placed in the low profile PCR tubes (Bio-Rad Cat#: TSL-0851) and filled with reaction master mix. All of the sample solid phases had triplicates and were lacking aptamers in/on them to test their ability to work in

native UDAR. Results of the reaction are presented in **Figure 3.8** which plots the averaged fluorescence of the triplicates each sample had with respect to time.

In-house (CDI) membrane resulted in very high initial fluorescence (~22,000) and commercial membrane also had high initial fluorescence (~15,000). Compared to the control (No Solid Phase), both membrane samples did not result in a high signal increase after the second phase. In-house (CDI) membrane most likely absorbed SYBR GREEN II and resulted in a high initial fluorescence, during aptamer immobilization on membranes, blank in-house (CDI) membranes resulted in unusually high fluorescence values as well. Submerging the whole membrane punch into a solution that has SYBR resulted in a high amount of nonspecific SYBR/Cellulose interaction that resulted in a high fluorescence at the start of the reaction. Commercial (SAM2 Biotin Capture) membrane also resulted in a high initial fluorescence, but this is most likely due to the autofluorescent nature of the commercial membranes.

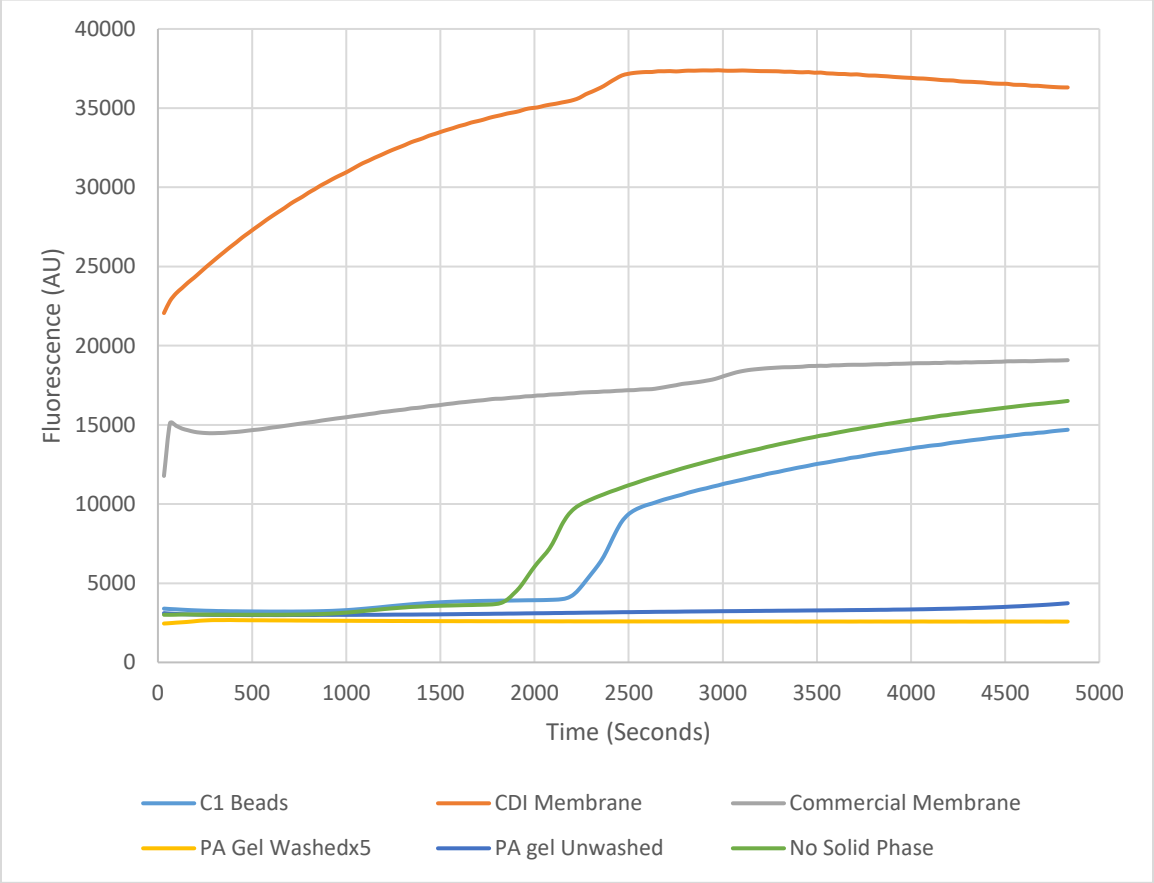

Figure 3.8: UDAR reaction conducted with different solid phases in the tubes. Data shows the change in fluorescence of the samples with respect to time.

Autofluorescent nature of the commercial (SAM2 Biotin Capture) membranes was investigated further using the EVOS FL Auto Imaging System (ThermoFisher). 3 mm punches of in-house (CDI) membranes and commercial (SAM2 Biotin Capture) membranes were wetted with 5 uL PBS and 5 uL PBS with 1 mg/mL BSA imaged with Light Intensity: 100 using the GPF Channel. Bar chart representing the background RFU levels of the membrane samples were represented in **Figure 3.9**. Samples 1 and 3 represent the in-house membranes and commercial membranes, respectively, that are wetted with PBS. Samples 2

and 4, which has a black outline, represents the in-house membranes and commercial membranes, respectively, that are wetted with 1 mg/mL BSA added PBS.

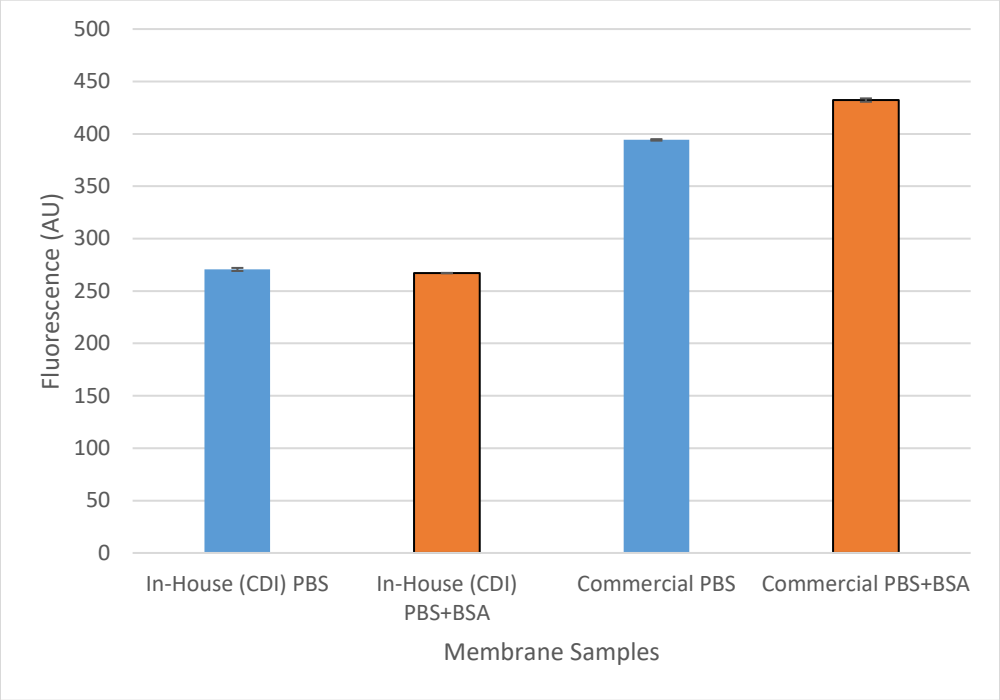

Figure 3.9: Average background fluorescence of the membrane samples represented in this bar chart.

Average background fluorescences for CDI membrane was washed with PBS were 270.57 ± 1.47 and commercial membrane were 394.91 ± 1.61. Commercial membranes have 45.7% more background fluorescence than the in house membrane samples. Addition of BSA seems to increase the background RFU values of the commercial membranes to 432.24 ± 1.61. This proves the autofluorescence of the commercial membranes. In-house membranes and commercial membranes have a slight increase in their fluorescence that

resembles the exponential phase of UDAR around ~2500 and 3000 seconds respectively. This suggests reaction is running but the membranes are interfering with the qPCR instrument's ability to measure the fluorescence.

C1 beads do not fully inhibit the UDAR as seen with the polyacrylamide gel slugs but slow the exponential phase of the reaction by ~380 seconds. They were observed to aggregate on the bottom of the tube at the end of the run. Ideally, beads should be dispersed in the solution.

Both washed and unwashed hollow polyacrylamide gel slugs seem to interfere with the reaction. As stated above, there are two possible foreseen reasons. First one is the inhibition of the UDAR reaction due to the introduction of the porous gel slug. The second one is, more possibly, bleeding of the chemicals that are in gel slugs that leads to inhibition.

To investigate the possible inhibition of the UDAR reaction, the reaction was run for 300 cycles, double the number of cycles from the usual reaction. **Figure 3.10** shows the fluorescence values of the UDAR reaction with respect to time. Washed gel slugs were washed three times with 100 µL TE buffer and conditioned (incubated) in 100 µL NEBuffer™ 3.1, no solid phase is the control where there was no PA gel in the tube.

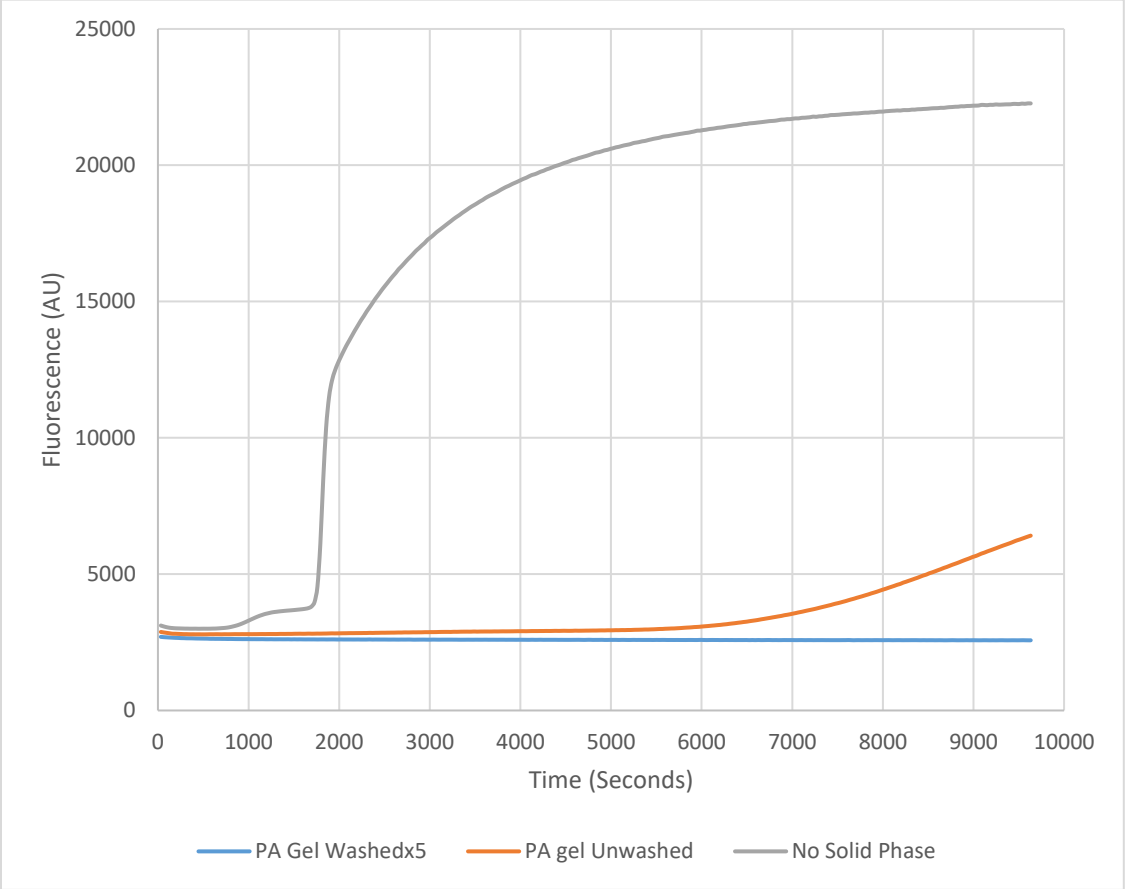

Figure 3.10: UDAR reaction conducted for twice longer. Data shows the fluorescence of the samples with respect to time.

This proves that reaction inhibition is highly unlikely due to diffusion limitation caused by the porous PA gel structure. As mentioned before, gel slugs were cast to be hollow specifically to reduce the length that reaction reagents and products need to diffuse through. One of the replicates for unwashed PA gel slugs resulted in an increase in RFU. This behavior has not been replicated and the reasons for this were unknown. Next step was to investigate the chemicals that are used in the production of the gel slugs. NanoDrop 1000 UV Spectrometer measurements (**Table 3.1)** showed that there were contaminants in the washing supernatant of

the hollow gel slugs. Three chemicals were used in the production of the gels. These Chemicals are 4 X AB, APS, and TEMED. 4 X AB is the monomer/crosslinker solution, APS is the oxidant and TEMED is the catalyzer. These chemicals bleed into the reaction mix (even after gel slugs being washed) and in a concentration currently unknown to us. To replicate the chemicals that are in the reaction mix, stock chemicals that were used in the production of the hollow gel slugs were added into the reaction mix to have a final dilution of 1:1000. **Figure 3.11** shows the change in fluorescence with respect to the time of the samples when the reaction is spiked with chemicals that are present in the PA gel slugs.

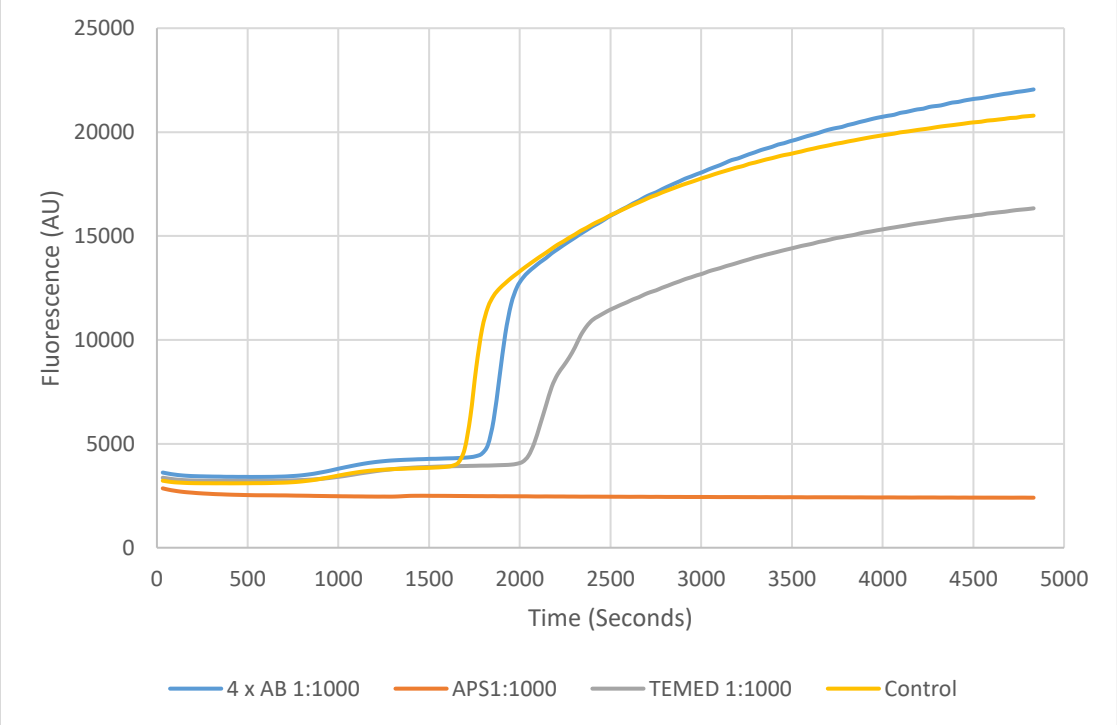

Figure 3.11: UDAR with PA gel chemicals spiked in the reaction mix. Data shows the fluorescence of the samples with respect to time.

Figure 3.11 shows clearly that at 1:1000 dilution, APS fully inhibits the reaction. AB mixture appears to slow the reaction while TEMED reduced the signal intensity and slightly slowed down the reaction. In the light of this data, APS concentration that does not inhibit the UDAR reaction needed to be determined. In the next experiment, different concentrations of APS were added into the reaction mix to figure out the minimum APS concentration that does not interfere with the reaction.

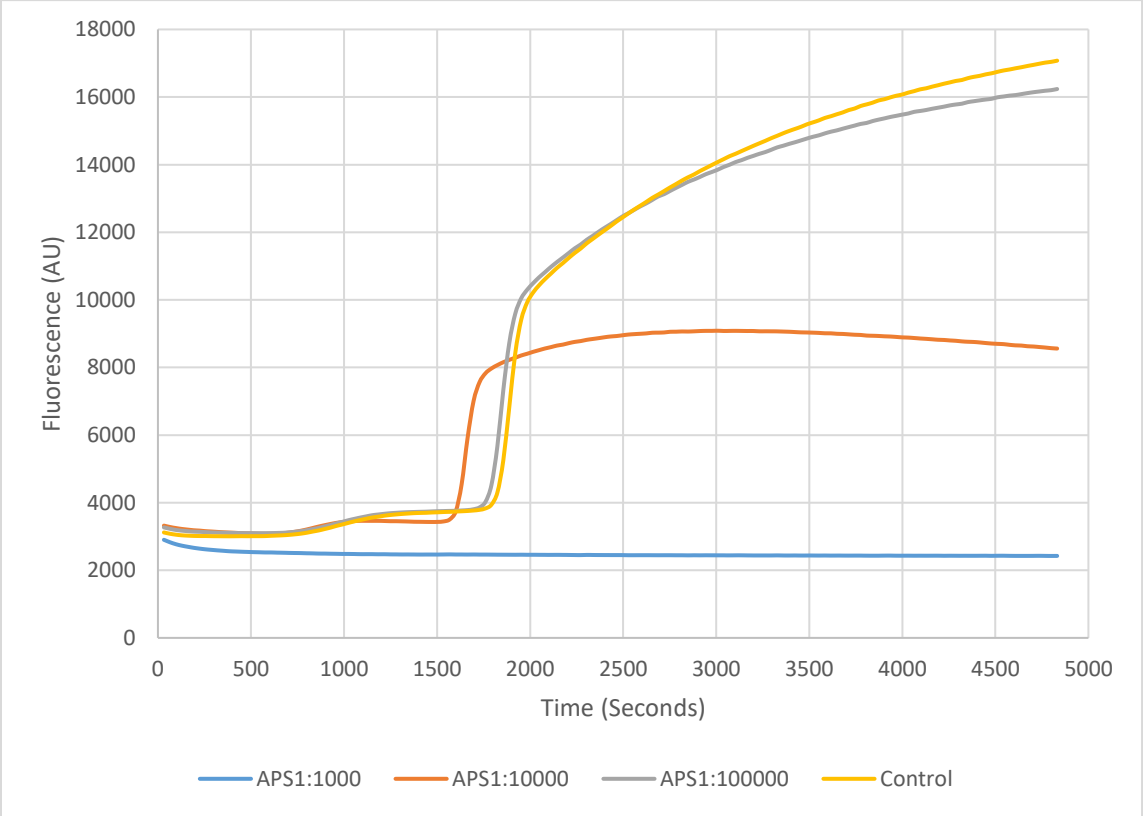

Figure 3.12: UDAR with various APS concentrations added in the reaction mix. Data shows the fluorescence of the samples with respect to time.

Figure 3.12 Shows the effects of the various APS concentrations on the UDAR reaction. It was previously established that 1:1000 dilution of the APS was inhibiting the reaction fully (**Figure 3.11**). APS solutions were serially diluted and added in the UDAR reaction mixes so that final concentrations of the APS in the reaction were 1:1000, 1:10,000 and 1:100,000. 1:100,000 dilution of APS did not exhibit any inhibition of the UDAR reaction. This data provides insightful knowledge about the washing conditions for the hollow gel slugs. Current formulation for the PA gel slugs requires 3 µL of APS in 100 µL of PA gel. Each hollow gel slugs were cast to have 10 µL of PA gel in it. This means each hollow gel slugs have 0.3 µL of APS in them. Washing and reconditioning of the gels seem to be ineffective to reduce APS concentrations since data represented in **Figure 3.8** and **Figure 3.10** still showed UDAR inhibition in the washed gel slug samples. In total, gel slugs used in those experiments were washed with 300 µL of TE buffer per gel slug. If washing of the gel slugs were fully effective, this would be equal to 1:1000 dilution of APS and in addition to washing, each of the gel slugs was conditioned in 100 µL NEBuffer 3.1 overnight. This method proves to be ineffective and to dilute 0.3 µL of APS that are in each of the gel slugs by 100,000-fold, ~3 mL buffer is required. So, for future experiments, each of the gel slugs should be washed/incubated in 3 mL of solution overnight to remove the APS from the gel slugs.

Overall Analysis of the Solid Phases

In this section, solid phases were evaluated based upon parameters that are important for the final assay. These parameters are DNA immobilization, ease of use, production time, price and UDAR (amplification) compatibility. Production time for the solid phases will be specific for each solid phase and will cover the time to prepare/manufacture each of the solid phases. The time it takes for conducting the assay will be excluded since it will be the same for all solid phase type. Price of each solid phase will represent how much a single unit costs, including reagent prices that were used during production. **Table 3.2** presents the values of these parameters.

Table 3.2: Values for the important assay parameters for each solid phase.

Name	C1 beads	In-House Membrane	Commercial Membrane	PA Gel
DNA Immobilization	95%	31%	77%	82%
Ease of Use	Easy	Moderate	Easy	Moderate
Production Time (minutes)	35	275	35	60
Price ($)	1.54	0.13	0.23	0.03
UDAR Compatibility	Yes	No	No	Yes*

The unit is the quantity of solid phase that goes into a single test tube during UDAR. For C1 beads it is 8.36 µL of stock, one 3 mm punch of in-house membrane (protocol showed in methods section is enough for 27 punches), one 3 mm punch for commercial membrane (one pack yields 864 punches), one

hollow PA gel slug that is cast using 10 µL of PA (protocol showed in methods section is enough for 10 hollow slugs). production time is the time it takes to produce 1 unit of the solid phase with 100 nM of aptamers immobilized on it. Price is the price of a unit solid phase, which includes the reagents that were used during production and excludes aptamer prices. UDAR compatibility is the ability of the solid phase to work during UDAR without interfering with the measurement and inhibiting reaction. There is a caveat with the PA gel, there is suggestive evidence that it is possible to use them in UDAR reaction if they are washed well enough, but this was not tested.

Protein Capture Using Modified Aptamers

For protein capture experiments, Dynabeads™ MyOne™ Streptavidin C1 beads were used. Compared to the other options (membranes and polyacrylamide gel slugs), C1 beads are the more user-friendly, less time consuming and easy to conduct the protein capture experiments. Protein capture experiment aims to test the modified and native aptamers ability to capture target proteins. As a control, A non-specific aptamer to target protein PBP2a immobilized beads (mCherry aptamer, GO5) and blank beads with no aptamer immobilized on to test the effects of nonspecific binding to the surface of the beads.

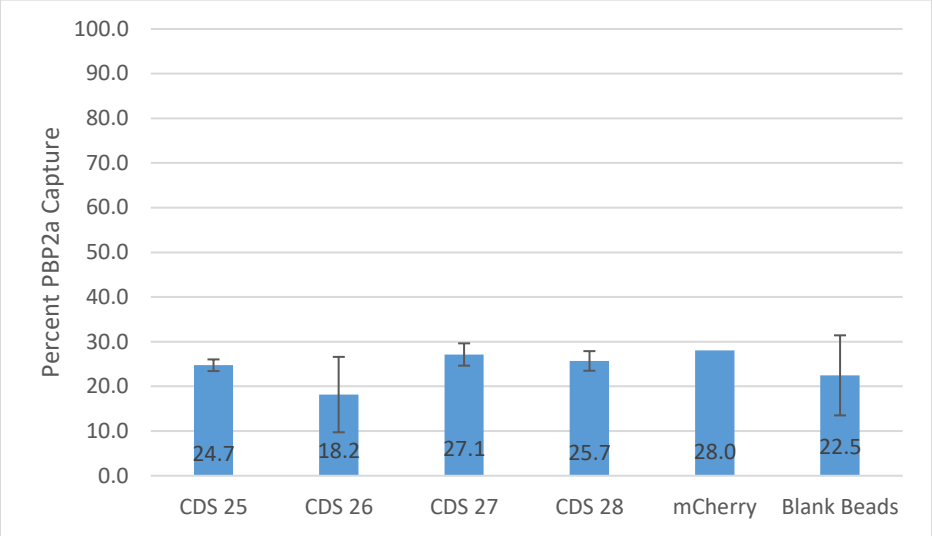

Figure 3.13: Percent of PBP2a captured (reduction) from the incubation supernatant when C1 beads with aptamers are incubated.

Data presented in **Figure 3.13** shows the percent of PBP2a captured from the sample solution with known concentration (100nM) by different sets of aptamers immobilized on C1 beads. This data suggests most of the non-specific binding likely occurs on the surface of the beads and all of the measurements are inside of each other's error bars, making it insignificant. Buffer solution these experiments were conducted had NF PBS and 0.01% Tween 20. It is evident that this buffer mixture is not sufficient enough to inhibit the nonspecific binding. It is important to prevent non-specific interactions between solid supports and target proteins for the protein capture/quantification experiments because, as presented in the **Figure 3.13** it prevents accurate quantification of the aptamers ability to bind and capture proteins.

Non-specific binding on the surface of the beads does not interfere with the assay's capability to detect antigens due to the structure switching nature of

the aptamers during UDAR. The signal that will be created by the amplification reaction will only be produced if aptamer has an open 3' end. Since the aptamers have their 3' ends closed initially and will only open after they bind to their target specifically, eliminates the worry of non-specific binding of the target antigens on the magnetic beads surface for the final assay. However, during characterization experiments, specifically in protein capture/quantification experiments, it is evident that there is a need for a blocking buffer.

For future experiments, a blocking buffer that contains Tween-20, BSA, fish gelatin and casein could be made. Preliminary tests with BSA as an addition to the washing/blocking buffer did not decrease the non-specific binding. The surface of the beads also contains streptavidin proteins, so in addition to the surface/protein interaction, there are protein-to-protein interactions as well. This requires a reagent in blocking buffer that would specifically prevent protein/protein interaction. Surface properties of all three solid phases are different from each other. For example, C1 beads are negatively charged and hydrophilic, so surface properties of the solid supports also need to be taken into consideration. Casein and fish gelatin are good leads that might satisfy these needs. Finally, other label-free strategies such as Surface Plasmon Resonance (SPR) can be used to study binding kinetics and thermodynamics of modified and unmodified aptamers.

Amplification Reaction

PBP2a aptamers were amplified using UDAR reaction to test the aptamers' compatibility with the amplification reaction. No solid phase was present in this reaction. Equal concentrations, 10 nM, or aptamer, transduction templates, and PBP2a were used. PBP2a aptamers (CDS0025, CSD0026, CSD0027 and CDS0028) were all tested. The results for CDS0026 are shown below.

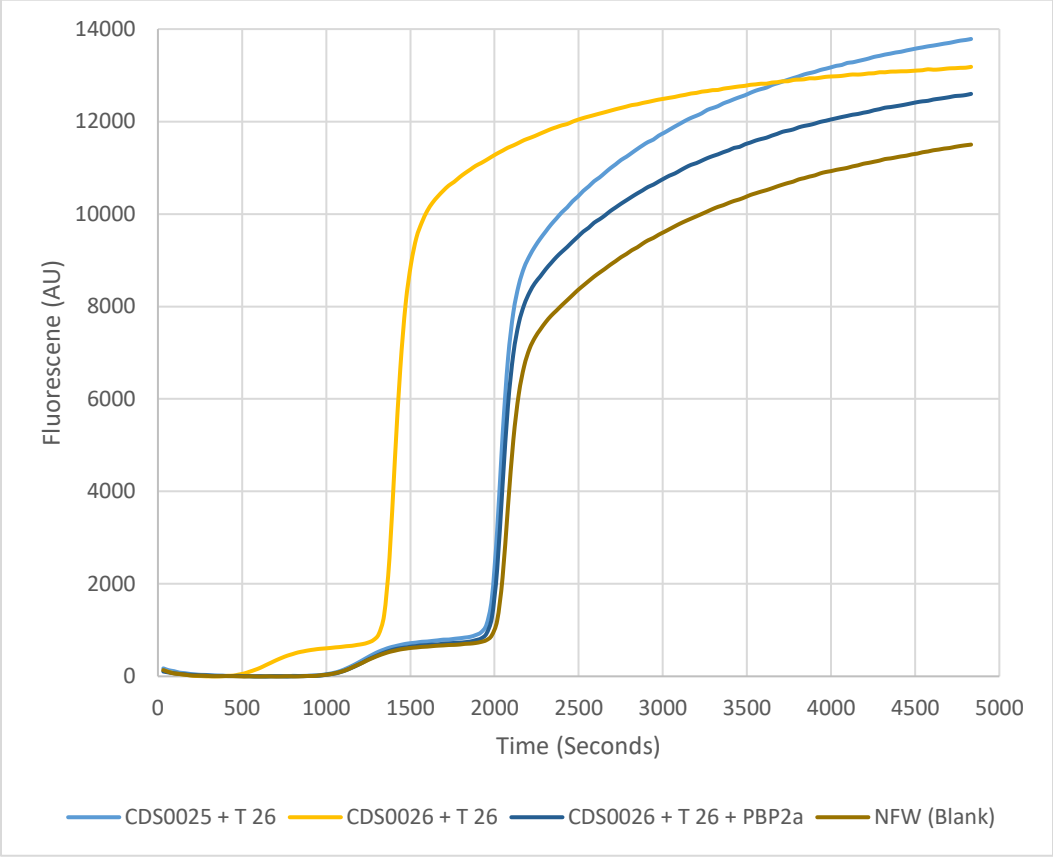

Figure 3.14: Change in fluorescence of the aptamer samples during UDAR. Raw data was analyzed using a MATLAB code that background corrects the data.

Figure 3.14 shows the change in fluorescence of the aptamer samples that were amplified using UDAR. Three controls were present in this experiment, native aptamer with no 3' complementary and a transduction template (CDS0025 + T 26), modified aptamer with specific transduction template (CDS0026 + T 26) and negative control with UDAR reaction mix with no added aptamers, transduction templates and proteins (NFW (Blank)). NFW (Blank) control amplifies non-specifically with time, which is a common feature of isothermal amplification reactions. It will be used as a baseline for other controls and sample (CSD0026 + T 26 + PBP2a). Controls and samples are compared to the NFW (blank) control to see the effects of these reagents in the reaction. **Table 3.3** shows the Inflection points of the first phase and the second phase of the reaction. Values presented in this table were calculated using a MATLAB code which analyzes the raw data (taking the derivative) and determines the time where the first phase of the reaction and second phase of the reaction happens.

Table 3.3: Shows the average inflection points of the UDAR amplification of aptamer CDS0026. These values were calculated using a MATLAB code that processes the raw data and calculates the inflections points of the two phases of the reaction.

Name	CDS0025 + T 26	CDS0026 + T 26	CDS0026 + T 26 + PBP2a	NFW (Blank)
Average Inflection 1 (s)	1216	663	1226	1211
Average Inflection 1 (s) SD	4	3	1	15
Average Inflection 2 (s)	2034	1414	2056	2095
Average Inflection 2 (s) SD	9	4	4	10
Average Max derivative 1 RFU/s)	53	49	50	45

Average Max derivative 2 (RFU/s)	1113	1424	1113	918
Average Plateau 1 (RFU)	688	560	601	557
Average Plateau 2 (RFU)	11627	12278	11070	9843

Addition of the CDS0026 and T 26 seem to speed up the reaction. The time it takes for the reaction to reach to the maximum, the first derivate equals to zero, is 663 ± 3 seconds for the first phase and 1414 ± 4 seconds for the second phase. Negative control resulted in its max first phase at 1211 ± 15 seconds and max the second phase at 2095 ± 10 seconds. Addition of target protein PBP2a seems to slow the first phase of the reaction by 563 seconds and second phase by 642 seconds, making it more relatable with a negative control that amplified non-specifically similar to the aptamer with a non-specific transduction template; which also resulted in behavior close to the negative control.

Experiments with other PBP2a aptamers (CSD0027, CDS0028, CDS004, CDS0041) also followed similar trends represented in **Figure 3.14** and **Table 3.2**. MATLAB code could not analyze some of these experiments' data due to not being able to detect the peaks due to reactions not showing a clear biphasic behavior. The code was written to detect and analyze data with clear biphasic behavior, any deviation usually results in an error that prevent the analysis.

It is evident that the presence of transduction templates causes non-specific amplification. In order to get accurate results, it is important to wash away any transduction templates that are not base paired with the aptamers.

During the trial phase, a sample with an unknown amount of targets will require the addition of excess amounts of transduction templates and presence of unbound transduction templates to aptamers that capture the target will result in inaccurate analyte concentration. To wash away the unbound transduction templates, a solid phase is required. It is important to identify a solid phase that is compatible with the UDAR and easy to work with during washing and protein capture/quantification experiments. In future experiments addition of a non-specific protein should be investigated to understand the reaction inhibition (slowing down) caused by target protein. At this state the reason for this behavior is unclear, it could be either because protein interacted with the aptamer or buffer used in lyophilization had adverse effects on the reaction.

CHAPTER FOUR

CONCLUSIONS

This thesis describes preliminary studies to inform the development of a protein detection assay. Important aspects of the assay were investigated, and the results here produced recommendations for assay design. Structure switching capabilities of the aptamers were investigated by designing aptamer beacons. Aptamer beacons v5 and v6 did not result in a significant change in their fluorescence in the presence of their target protein, VEGF. This suggests aptamer beacons did not open. Three different types of solid phases were investigated on their ability to immobilize DNA: ease of use, price per unit and compatibility with UDAR. Out of all three types of solid, phases, only the C1 beads had the highest aptamer immobilization (~95.1%) and it is compatible with UDAR. For membranes, 2 options were investigated CDI activated cellulose membranes that were made in-house and commercially available biotin capture membranes. In-house membranes resulted in high of variability in their DNA binding capabilities (32.1 ± 38.4%) and they were proven to be incompatible with UDAR since they non-specifically interact with SYBR Dyes. Commercial membranes had better performance than the in-house membranes in terms of DNA immobilization abilities (77.2 ± 7.3%) however, they are also incompatible with UDAR due to their autofluorescent nature. Finally, PA gels captured 82.4 ± 9.18% of the DNA molecules by crosslinking into the polymer. PA gels seem to

fully inhibit the UDAR, and gel slugs that were washed and conditioned in reaction buffer were also inhibiting the reaction. Further investigation showed APS inside of the gel slugs were the culprit for the reaction inhibition and in order to make PA gel slugs compatible with UDAR, they should be washed extensively. Further experimentation showed that each 10 µL hollow gel slug needs to be washed with 3 mL buffer. As an accidental finding, APS seems to accelerate the reaction, however further studies need to be conducted to validate this behavior. Protein capture experiments were conducted with C1 beads. When the performance of the aptamer immobilized beads was compared to the blank and non-specific aptamer controls, it is evident that results were inconclusive. Non-specific binding of proteins to the surface is likely to be the reason for this. Amplification of the aptamers showed that there is a need for washing of the unbound transduction templates in order to have accurate detection of the target analyte.

Future work for this assay should include a detailed investigation of aptamer beacons. Aptamer beacons with protein binding site initially double stranded on to one of its ends should be investigated. Products of the UDAR which ran with membranes should be analyzed using an SDS PAGE gel to show addition of membranes only effect the measurement of fluorescence and not the UDAR. An alternative hydrogel (Polyethylene Glycol, PEG) to the PA should be investigated. Even though PA gel slugs were cast to be hollow, having bigger pore size is an advantage and alternative hydrogel should have pores sized

bigger than 50 nm to allow reagent to easily diffuse in and out of the reaction. This can be achieved by reducing the monomer and crosslinker in the PA gel recipe. Protein capturing experiments should be conducted with aptamer bound PA gel slugs to evaluate the performance of the gel slugs. Further investigation is required to prove the validity of washing PA gel slugs with 3 mL of buffer to make them UDAR compatible. 3D printed molds for PA gel casting can be printed to make gel casting process easier and more reproducible. Finally, in order to be able to successfully determine the aptamers' binding capabilities, a blocking buffer should be identified, and using different solid phases will require different blocking buffers. SPR can also be used to precisely determine the aptamer's ability to bind its target without fluorescence detection. This will help the aptamer characterization and optimization tremendously.

The results presented and discussed in this thesis lays the foundation for a novel protein detection assay and investigated some of its key components. This assay has the potential to be used in low-resource settings and may be a competitor to the current protein detection methods due to aptamers cheap and robust nature. In the future number of targets could be expanded by changing the aptamer; for example, this assay can be used in forensic applications to detect various narcotic substances.

REFERENCES CITED:

[1] Urdea, M., et al. Requirements for high impact diagnostics in the developing world. Nature 444, 73-79 (2006).

[2] CMS.gov “National Health Expenditure 2017-2026” *NHE Fact Sheet* Feb. 2018

[3] Nimjee, Shahid M., et al. "Aptamers as therapeutics." Annual review of pharmacology and toxicology 57 (2017): 61-79.

[4] Zhou, Jiehua, and John Rossi. "Aptamers as targeted therapeutics: current potential and challenges." Nature Reviews Drug Discovery 16.3 (2017): 181.

[5] Jayasena, Sumedha D. "Aptamers: an emerging class of molecules that rival antibodies in diagnostics." Clinical chemistry 45.9 (1999): 1628-1650.

[6] Wilson, David S., and Jack W. Szostak. "In vitro selection of functional nucleic acids." Annual review of Biochemistry 68.1 (1999): 611-647.

[7] Engvall, Eva, and Peter Perlmann. "Enzyme-linked immunosorbent assay, ELISA: III. Quantitation of specific antibodies by enzyme-labeled anti-immunoglobulin in antigen-coated tubes." The Journal of Immunology 109.1 (1972): 129-135.

[8] Clark, Michael F., and A. N. Adams. "Characteristics of the microplate method of enzyme-linked immunosorbent assay for the detection of plant viruses." Journal of general virology 34.3 (1977): 475-483.

[9] Özay, Burcu, et al. "First Characterization of a Biphasic, Switch-like DNA Amplification." Analyst (2018).

[10] Nutiu, Razvan, and Yingfu Li. "Structure-switching signaling aptamers." Journal of the American Chemical Society 125.16 (2003): 4771-4778.

[11] Binnicker, M.J. Multiplex Molecular Panels for Diagnosis of Gastrointestinal Infection: Performance, Result Interpretation, and Cost-Effectiveness. Journal of clinical microbiology 53, 3723-3728 (2015).

[12] Pepe, M. S., et al. “Phases of Biomarker Development for Early Detection of Cancer.” JNCI Journal of the National Cancer Institute, vol. 93, no. 14, 2001, pp. 1054–1061., doi:10.1093/jnci/93.14.1054.

[13] White, Ryan J., et al. "Optimization of electrochemical aptamer-based sensors via optimization of probe packing density and surface chemistry." Langmuir 24.18 (2008): 10513-10518.

[14] Cerchia, Laura, et al. “Cell-Specific Aptamers for Targeted Therapies.” Methods in Molecular Biology Nucleic Acid and Peptide Aptamers, 2009, pp. 59–78., doi:10.1007/978-1-59745-557-2_5.

[15] Ng, Eugene WM, et al. "Pegaptanib, a targeted anti-VEGF aptamer for ocular vascular disease." Nature reviews drug discovery 5.2 (2006): 123.

[16] Herr, Joshua K., et al. "Aptamer-conjugated nanoparticles for selective collection and detection of cancer cells." Analytical Chemistry 78.9 (2006): 2918-2924.

[17] Xiao, Yi, et al. "Label-free electronic detection of thrombin in blood serum by using an aptamer-based sensor." Angewandte Chemie 117.34 (2005): 5592-5595.

[18] Watkins, Herschel M., et al. "Effects of crowding on the stability of a surface-tethered biopolymer: an experimental study of folding in a highly crowded regime." Journal of the American Chemical Society 136.25 (2014): 8923-8927.

[19] Dill, Ken A. "Dominant forces in protein folding." Biochemistry 29.31 (1990): 7133-7155.

[20] Abu-Lail, Nehal I., and Terri A. Camesano. "Role of Ionic Strength on the Relationship of Biopolymer Conformation, DLVO Contributions, and Steric Interactions to Bioadhesion of P seudomonas p utida KT2442." Biomacromolecules 4.4 (2003): 1000-1012.

[21] Watkins, Herschel M., et al. "Entropic and electrostatic effects on the folding free energy of a surface-attached biomolecule: an experimental and theoretical study." Journal of the American Chemical Society 134.4 (2012): 2120-2126.

[22] Hamaguchi, Nobuko, Andrew Ellington, and Martin Stanton. "Aptamer beacons for the direct detection of proteins." Analytical biochemistry 294.2 (2001): 126-131.

[23] Shaner, Nathan C., et al. "Improved monomeric red, orange and yellow fluorescent proteins derived from Discosoma sp. red fluorescent protein." Nature biotechnology 22.12 (2004): 1567.

[24] Hubalek, Zdenek. "Protectants used in the cryopreservation of microorganisms." Cryobiology 46.3 (2003): 205-229.

[25] Jeong, Haeyoung, et al. "Unveiling the hybrid genome structure of Escherichia coli RR1 (HB101 RecA+)." Frontiers in microbiology 8 (2017): 585.

[26] Ryan, Kenneth J., et al. "Stability of antibiotics and chemotherapeutics in agar plates." Applied microbiology 20.3 (1970): 447-451.

[27] Summers, David K. "The kinetics of plasmid loss." Trends in biotechnology 9.1 (1991): 273-278.

[28] Smith, M. Alex, and Michael J. Bidochka. "Bacterial fitness and plasmid loss: the importance of culture conditions and plasmid size." Canadian journal of microbiology 44.4 (1998): 351-355.

[29] Xiao, Yuhong, and Stuart N. Isaacs. "Enzyme-linked immunosorbent assay (ELISA) and blocking with bovine serum albumin (BSA)—not all BSAs are alike." Journal of immunological methods 384.1-2 (2012): 148-151.

[30] Win, Maung Nyan, Joshua S. Klein, and Christina D. Smolke. "Codeine-binding RNA aptamers and rapid determination of their binding constants using a direct coupling surface plasmon resonance assay." Nucleic acids research 34.19 (2006): 5670-5682.

[31] Lee, Hye-Jin, et al. "A sensitive method to detect Escherichia coli based on immunomagnetic separation and real-time PCR amplification of aptamers." Biosensors and Bioelectronics 24.12 (2009): 3550-3555.

[32] Lei, Pinhua, et al. "Determination of the invA gene of Salmonella using surface plasmon resonance along with streptavidin aptamer amplification." Microchimica Acta 182.1-2 (2015): 289-296.

[33] Kim, Yeon Seok, et al. "Isolation and characterization of DNA aptamers against Escherichia coli using a bacterial cell–systematic evolution of ligands by exponential enrichment approach." Analytical biochemistry 436.1 (2013): 22-28.

[34] Yildirim, Nimet, Feng Long, and April Z. Gu. "Aptamer based E-coli detection in waste waters by portable optical biosensor system." Bioengineering Conference (NEBEC), 2014 40th Annual Northeast. IEEE, 2014.

[35] Zhang, Congxiao, et al. "Whole-cell based aptamer selection for selective capture of microorganisms using microfluidic devices." Analytical Methods 7.15 (2015): 6339-6345.

[36] Kaur, Harleen, and Lin-Yue Lanry Yung. "Probing high affinity sequences of DNA aptamer against VEGF165." PLoS One 7.2 (2012): e31196.

[37] Nonaka, Yoshihiko, Koji Sode, and Kazunori Ikebukuro. "Screening and improvement of an anti-VEGF DNA aptamer." Molecules 15.1 (2010): 215-225.

[38] Gilbert, Sunny D., et al. "Thermodynamic and kinetic characterization of ligand binding to the purine riboswitch aptamer domain." Journal of molecular biology 359.3 (2006): 754-768.

[39] Neves, Miguel AD, et al. "Defining the secondary structural requirements of a cocaine-binding aptamer by a thermodynamic and mutation study." Biophysical chemistry 153.1 (2010): 9-16.

[40] Bishop, G. Reid, et al. "Energetic basis of molecular recognition in a DNA aptamer." Biophysical chemistry 126.1-3 (2007): 165-175.

[41] Zuker, Michael. "Mfold web server for nucleic acid folding and hybridization prediction." Nucleic acids research 31.13 (2003): 3406-3415.

[42] Waugh, Allison, et al. "RNAML: a standard syntax for exchanging RNA information." Rna 8.6 (2002): 707-717.

[43] ZUKER, MICHAEL, and ANN B. JACOBSON. "Using reliability information to annotate RNA secondary structures." Rna 4.6 (1998): 669-679.

[44] Rohr, Ulrich-Peter, et al. "The value of in vitro diagnostic testing in medical practice: a status report." PLoS One 11.3 (2016): e0149856.

[45] Rifai, Nader, Michael A. Gillette, and Steven A. Carr. "Protein biomarker discovery and validation: the long and uncertain path to clinical utility." Nature biotechnology 24.8 (2006): 971.

[46] Urdea, M., et al., Requirements for high impact diagnostics in the developing world. Nature, 2006: p. 73.

[47] Watson, J. D., & Crick, F. H. (1953). Molecular structure of nucleic acids. Nature, 171(4356), 737-738.

[48] Green, N. M. (1963). Avidin. 3. The nature of the biotin-binding site. Biochemical Journal, 89(3), 599.

[49] Stöllner, D., Scheller, F. W., & Warsinke, A. (2002). Activation of cellulose membranes with 1, 1′-carbonyldiimidazole or 1-cyano-4-dimethylaminopyridinium tetrafluoroborate as a basis for the development of immunosensors. Analytical biochemistry, 304(2), 157-165.

[50] Liu, W., Huang, S., Liu, N., Dong, D., Yang, Z., Tang, Y., ... & Zou, D. (2017). Establishment of an accurate and fast detection method using molecular beacons in loop-mediated isothermal amplification assay. Scientific reports, 7, 40125.

[51] Stellwagen, N. C. (1998). Apparent pore size of polyacrylamide gels: Comparison of gels cast and run in Tris-acetate-EDTA and Tris-borate-EDTA buffers. Electrophoresis, 19(10), 1542-1547.

[52] Yang, L., & Ellington, A. D. (2008). Real-time PCR detection of protein analytes with conformation-switching aptamers. Analytical biochemistry, 380(2), 164-173.

[53] Tong, J., & Anderson, J. L. (1996). Partitioning and diffusion of proteins and linear polymers in polyacrylamide gels. Biophysical journal, 70(3), 1505-1513.

[54] LaBarre, P., Gerlach, J., Wilmoth, J., Beddoe, A., Singleton, J., & Weigl, B. (2010, August). Non-instrumented nucleic acid amplification (NINA): instrument-free molecular malaria diagnostics for low-resource settings. In 2010 Annual International Conference of the IEEE Engineering in Medicine and Biology (pp. 1097-1099). IEEE.

[55] Liao, A. M., Pan, W., Benson, J. C., Wong, A. D., Rose, B. J., & Caltagirone, G. T. (2018). A Simple Colorimetric System for Detecting Target Antigens by a Three-Stage Signal Transformation–Amplification Strategy. Biochemistry, 57(34), 5117-5126.